Development 139, 4383-4394 (2012) doi:10.1242/dev.083352

Frizzled 2 and frizzled 7 function redundantly in convergent extension and closure of the ventricular septum and palate: evidence for a network of interacting genes

Huimin Yu[1], Xin Ye[1,*], Nini Guo[1,‡] and Jeremy Nathans[1,2,3,4,§]

SUMMARY

Frizzled (Fz) 2 and Fz7, together with Fz1, form a distinct subfamily within the Frizzled family of Wnt receptors. Using targeted gene deletion, we show that: *Fz7*$^{-/-}$ mice exhibit tail truncation and kinking with 100% penetrance and ventricular septal defects (VSDs) with ~15% penetrance; *Fz2*$^{+/-}$*;Fz7*$^{-/-}$ mice exhibit VSDs with ~50% penetrance and cleft palate with less than 10% penetrance; and *Fz2*$^{-/-}$*;Fz7*$^{-/-}$ mice exhibit convergent extension defects and mid-gestational lethality with 100% penetrance. When *Fz2* and/or *Fz7* mutations are combined with mutations in *Vangl2*, *Dvl3*, *Wnt3a*, *Wnt5a* or *Wnt11*, an increased frequency of VSDs is observed with *Dvl3*, *Wnt3a* and *Wnt11*; an increased frequency of palate closure defects is observed with *Vangl2*; and early lethality and enhanced tail shortening are observed with *Wnt5a*. To assess the signaling pathways that underlie these and other Frizzled-mediated genetic interactions, we used transfected mammalian cells to analyze (1) canonical Wnt signaling induced by all pairwise combinations of the ten mouse Frizzleds and the 19 mouse Wnts and (2) localization of each Frizzled at cell-cell junctional complexes formed by mouse Celsr1, a likely indicator of competence for planar cell polarity signaling. These in vitro experiments indicate that Fz2 and Fz7 are competent to signal via the canonical pathway. Taken together, the data suggest that genetic interactions between *Fz2*, *Fz7* and *Vangl2*, *Dvl3* and Wnt genes reflect interactions among different signaling pathways in developmental processes that are highly sensitive to perturbations in Frizzled signaling.

KEY WORDS: Fz2, Fz7, Convergent extension, Planar cell polarity, Wnt signaling

INTRODUCTION

Frizzled receptors are found throughout the animal kingdom, where they play central roles in controlling cell proliferation, movement and polarity. Frizzleds function as the principal receptors for the Wnt family of ligands and they couple to at least three distinct intracellular signaling pathways: the canonical Wnt pathway, the planar cell/tissue polarity (PCP) pathway, and the calcium pathway (van Amerongen and Nusse, 2009). The first two pathways are highly conserved between vertebrates and insects; the third has been studied principally in vertebrates. Canonical Wnt signaling features a co-receptor (Lrp5 or Lrp6 in mammals) that suppresses the constitutive proteolysis of β-catenin, which then migrates to the nucleus and, in conjunction with LEF/TCF family members, controls transcription of target genes. PCP signaling has been most extensively studied in epithelia, where it controls cytoskeletal organization via a set of asymmetrically positioned plasma membrane protein complexes that mediate vectorial communication between neighboring cells. These complexes are composed of Frizzled together with several other conserved PCP membrane proteins, including Stan/Fmi/Celsr and Vang/Vangl family members (Goodrich and Strutt, 2011; Gray et al., 2011).

[1]Department of Molecular Biology and Genetics, [2]Department of Neuroscience, [3]Department of Ophthalmology and the [4]Howard Hughes Medical Institute, Johns Hopkins University School of Medicine, Baltimore, MA 21205, USA.

*Present address: Whitehead Institute for Biomedical Research, Cambridge, MA 02142, USA
‡Present address: U.S. Food and Drug Administration, Building 29A, Room 1C20, 29 Lincoln Drive, Bethesda, MD 20892, USA
§Author for correspondence (jnathans@jhmi.edu)

Accepted 31 August 2012

Targeted loss-of-function mutations in the mouse have revealed developmental phenotypes for most of the ten Frizzled receptor genes. In many cases, partial redundancy is observed, especially among Frizzleds that are closely related in sequence. Redundant pairs include frizzled (Fz) 1 and Fz2, Fz3 and Fz6, Fz4 and Fz8, and Fz5 and Fz8 (Wang et al., 2006b; Yu et al., 2010; Ye et al., 2011; Liu et al., 2012). *Fz3*$^{-/-}$ and *Fz6*$^{-/-}$ mice exhibit phenotypes that appear the most PCP-like, as judged by their similarities to PCP phenotypes in *Drosophila* or to phenotypes caused by mutations in other core PCP genes in mice (e.g. *Celsr1-3* and *Vangl2*). These include defects in CNS axon guidance (*Fz3*) and hair follicle orientation (*Fz6*) (Wang et al., 2002; Wang et al., 2006a; Lyuksyutova et al., 2003; Guo et al., 2004). *Fz3*$^{-/-}$*;Fz6*$^{-/-}$ embryos additionally exhibit a fully open neural tube (craniorrhachischisis) and defects in inner ear sensory hair cell orientation (Wang et al., 2006b), as do *Vangl2*$^{Lp/Lp}$ embryos and *Vangl1*$^{+/-}$*;Vangl2*$^{Lp/+}$ embryos (Strong and Hollander, 1949; Torban et al., 2008). By contrast, Fz4 appears to act predominantly or exclusively via canonical Wnt signaling to control retinal vascularization (Xu et al., 2004). Fz4 also functions redundantly with Fz8 in kidney development, with *Fz4*$^{-/-}$*;Fz8*$^{-/-}$ embryos exhibiting renal hypoplasia (Ye et al., 2009; Ye et al., 2011). Interestingly, in cell culture, Fz4 can activate both the canonical Wnt signaling pathway and the non-canonical Rho pathway. For most mammalian Frizzled genes, the question of which signaling pathway accounts for which developmental function remains open.

The present study focuses on *Fz2* and *Fz7*, which, together with *Fz1*, form a distinct subfamily among mammalian Frizzled genes. As noted above, *Fz1* and *Fz2* are partially redundant. *Fz1*$^{-/-}$*;Fz2*$^{-/-}$ embryos exhibit fully penetrant defects in palate closure and incomplete, but highly penetrant, ventricular septal defects (VSDs) (Yu et al., 2010). On a *Vangl2*$^{Lp/+}$ background, loss of *Fz1* and/or

Fz2 greatly increases the frequency of neural tube defects and loss of *Fz2* enhances the misorientation of inner ear sensory hair cells. These data suggest an interaction between PCP signaling and Fz1/Fz2 signaling – either a direct role of *Fz1* and *Fz2* in PCP signaling or an additive effect of compromised PCP signaling mediated by *Vangl2* and non-PCP signaling mediated by *Fz1* and *Fz2*. In the present study, we show that *Fz7* is highly redundant with *Fz2*, we characterize the $Fz2^{-/-};Fz7^{-/-}$ embryonic lethal phenotype, we explore genetic interactions between *Fz2*, *Fz7* and a series of canonical and non-canonical signaling genes, and we systematically compare the canonical and PCP signaling competence of all ten Frizzled family members in cell culture assays to address the potential of each Frizzled to mediate signaling in one or both pathways.

MATERIALS AND METHODS

Construction of $Fz7^{-/-}$ mice

The *Fz7* gene targeting vector replaced the intronless *Fz7* coding region with DNA coding for a nuclear-localized *lacZ* followed by a *LoxP-PGK-neo-LoxP* cassette (supplementary material Fig. S1). ES cell targeting, Southern blot screening, blastocyst injections and excision of the *LoxP-PGK-neo-LoxP* cassette were performed as described (Yu et al., 2010). PCR primers for the endogenous *Fz7* gene are 5′-ATGGCGTCGCTTCTACCACAGACTCAGCCACAGC-3′ and 5′-ACAACCACTTGCCTTGCAGCAGGGGATTGGACTC-3′. Primers for the knock-in $Fz7^{lacZ}$ allele are 5′-GCCTCCCTGTATCCAAGCCTCTCCCCAGCG-3′ and 5′-CATCAACATTAAATGTGAGCGAGTAACAACCCG-3′.

Mouse lines and husbandry

$Fz2^{-/-}$ mice were described by Yu et al. (Yu et al., 2010). The following lines were obtained from the Jackson Laboratories: $Vangl2^{Lp}$ (Strong and Hollander, 1949); $Wnt3a^{+/-}$ (Takada et al., 1994); $Wnt5a^{+/-}$ (Yamaguchi et al., 1999); and $Dvl3^{+/-}$ (Etheridge et al., 2008). The $Vangl2^{Lp}$ allele was typed by PCR and sequencing as described (Yu et al., 2010). Mice were maintained on a mixed C57BL/6 × Sv129 background.

Wnt and Frizzled plasmids

Wnt and Frizzled open reading frames for expression in mammalian cells were purchased from Open BioSystems, identified by screening cDNA libraries, or obtained by PCR amplification of genomic DNA (for Frizzled coding regions lacking introns), and inserted into vectors with a cytomegalovirus immediate-early enhancer/promoter. An optimal translation initiation context (CCACCATG) was added by PCR to each Wnt and Frizzled coding region. For the Celsr1 colocalization experiments, a monoclonal antibody (mAb) 1D4 epitope [the C-terminus of bovine rhodopsin (Molday and MacKenzie, 1983)] was added to the C-terminus of each Frizzled coding region. All coding regions were fully sequenced to rule out spurious mutations.

Canonical Wnt signaling assay

A stable HEK293 cell line expressing a firefly luciferase reporter under the control of a minimal promoter and seven tandem LEF/TCF binding sites [Super Top Flash (STF) cells (Xu et al., 2004)] was transiently transfected in triplicate using FuGENE 6 (Roche) with expression plasmids encoding Wnt (50 ng), Frizzled (50 ng) and Lrp5 (5 ng), together with 1 ng *Renilla* luciferase expression plasmid and empty vector to bring the total DNA to 150 ng per well in a 24-well tray. Control transfections were performed as above, but with either the Wnt or Frizzled plasmids omitted. Luciferase activity was determined 48 hours post-transfection, and these values were corrected for any well-to-well variations in transfection efficiency and/or cell number by dividing each by the internal control *Renilla* luciferase activity. A second calculation normalized the canonical Wnt signaling activity from cells transfected with Wnt+Fz+Lrp5 relative to the canonical Wnt signaling activity from cells transfected with Wnt+Lrp5 and Fz+Lrp5. This value was calculated for each Wnt and Frizzled combination as follows: (Wnt+Fz+Lrp5)/[(Wnt+Lrp5)+(Fz+Lrp5)]. For example, if a particular Wnt+Fz+Lrp5 combination produced 1000 luciferase units and the individual Wnt+Lrp5 and Fz+Lrp5 samples produced 20 and 80 luciferase units, respectively, then the normalized value would be 1000/(20+80)=10.

For hierarchical clustering of Wnts and Frizzleds based on their mutual interactions, calculations were performed with both normalized and non-normalized data sets (as defined above). Using the $\log_2$ data sets, the mean Wnt+Fz+Lrp5 luciferase activity levels for each of the 19 Wnts was calculated and subtracted from the ten individual Wnt+Fz+Lrp5 luciferase activity values for that particular Wnt. The mean subtracted values were used for unsupervised hierarchical clustering using Pearson's correlation (Spotfire, Tibco).

Histology

Paraffin embedding and sectioning, anti-PECAM staining of embryo whole-mounts and X-Gal staining followed standard protocols (Ye et al., 2009; Yu et al., 2010). For plastic sections, yolk sacs were fixed with paraformaldehyde (PFA) and glutaraldehyde, osmicated, and embedded in Spurr's resin.

Transfection and immunostaining of Madin-Darby canine kidney (MDCK) cells

The plasmid coding for the mouse Celsr1-GFP fusion was a kind gift of Dr Elaine Fuchs (Rockefeller University, New York, USA), and mouse Celsr2-HA was a kind gift of Dr Tadashi Uemura (Kyoto University, Kyoto, Japan). MDCK cells were transfected with FuGENE 6 and imaged 2 days later using a Zeiss LSM700.

Immunostaining for cell surface protein

HEK293 cells (the parent cell line from which STF cells were derived) were seeded onto gelatin-coated coverslips and transiently transfected with plasmids coding for N-terminal 3×HA epitope-tagged Fz3 (3HA-Fz3), N-terminal 3×HA epitope-tagged Fz6 (3HA-Fz6), C-terminal rhodopsin epitope-tagged Fz3 (Fz3-1D4), or C-terminal rhodopsin epitope-tagged Fz6 (Fz6-1D4). The N-terminal tags were inserted between the end of the predicted signal peptide and the beginning of the ligand-binding cysteine-rich domain, with a duplication of four amino acids from the target Frizzled sequence flanking the site of 3×HA epitope insertion (SLFS for Fz3 and SLFT for Fz6). One day after transfection, coverslips were processed in one of two ways: (1) to visualize epitopes accessible exclusively from the extracellular space, living cells were stained with rabbit anti-3×HA antiserum or mouse mAb 1D4 in cell culture medium with 0.5% calf serum for 1 hour on ice, washed in ice-cold PBS, and then fixed with 4% PFA/PBS for 30 minutes on ice; and (2) to visualize epitopes in all locations, cells were fixed with 4% PFA/PBS for 30 minutes on ice, and immunostained with rabbit anti-3×HA antiserum or mouse mAb 1D4 in 0.3% Triton X-100/PBS/10% normal goat serum (NGS) overnight at 4°C and washed in 0.3% Triton X-100/PBS. After primary antibody binding, coverslips from both procedures were incubated in secondary antibodies and DAPI in 0.3% Triton X-100/PBS/10% NGS for 2 hours at room temperature. For all of the samples, transfections and immunostaining reactions were carried out in duplicate and in parallel. Confocal images of matched pairs of permeabilized and non-permeabilized samples were collected with identical parameter settings.

Microarray hybridization

Individual embryonic day (E) 8.5 embryos were stored at –80°C while their genotypes were determined from yolk sac DNA. For each RNA sample, two or three E8.5 embryos of identical Frizzled genotype but undetermined sex were pooled, and RNA was purified using Trizol (Invitrogen) and RNeasy (Qiagen) kits. Three biologically independent sets of $Fz7^{-/-}$ versus $Fz2^{-/-};Fz7^{-/-}$ embryo RNAs were hybridized to Affymetrix mouse genome 430 2.0 microarrays and the data analyzed using Spotfire. The microarray data are available at Gene Expression Omnibus with accession number GSE37221.

Statistics

Pairwise comparisons of phenotype frequencies were performed with 2×2 contingency tables and Fisher's exact test.

RESULTS

Targeted replacement of *Fz7* with *lacZ*

To eliminate *Fz7* function, we generated a mouse line carrying a targeted replacement of the *Fz7* coding region with the coding region of a nuclear-localized derivative of *E. coli* β-galactosidase (we refer to this allele equivalently as $Fz7^{lacZ}$ or $Fz7^{-}$; supplementary material Fig. S1). $Fz7^{lacZ/lacZ}$ mice are viable and fertile; their only apparent anatomical phenotype is a ~10% shorter tail with a distal kink, as discussed below. X-Gal staining of $Fz7^{lacZ/lacZ}$ embryos at E8.5 and E9.5 shows widespread expression of the *lacZ* reporter, including expression throughout the developing nervous system and somites. This pattern closely resembles the embryonic expression patterns observed for $Fz1^{lacZ}$ and $Fz2^{lacZ}$ alleles (Yu et al., 2010) (supplementary material Fig. S1).

As noted above, *Fz1*, *Fz2* and *Fz7* constitute a distinct branch of the Frizzled family of receptors (supplementary material Fig. S2), and *Fz1* and *Fz2* show partial redundancy (Yu et al., 2010). To explore the possibility of additional redundancies within this subfamily, we generated mice with various combinations of $Fz1^{-}$ and $Fz7^{-}$ alleles and $Fz2^{-}$ and $Fz7^{-}$ alleles. $Fz1^{-/-};Fz7^{-/-}$ mice are healthy and fertile but have a gray coat color, suggesting that these genes act redundantly in some aspect of melanocyte development, function or survival. Approximately 50% of $Fz2^{+/-};Fz7^{-/-}$ embryos have cardiac defects (described more fully below) and more than 50% of $Fz2^{+/-};Fz7^{-/-}$ embryos fail to survive postnatally; the surviving minority of $Fz2^{+/-};Fz7^{-/-}$ mice are viable and fertile. Genotyping of more than 100 progeny from an intercross among $Fz2^{+/-};Fz7^{-/-}$ mice revealed no $Fz2^{-/-};Fz7^{-/-}$ progeny at any postnatal age.

Early lethal phenotype in $Fz2^{-/-};Fz7^{-/-}$ embryos

An examination of mid-gestation embryos from $Fz2^{+/-};Fz7^{-/-}$ intercrosses showed growth retardation of $Fz2^{-/-};Fz7^{-/-}$ embryos starting at ~E8.5, with death at ~E10.5 (Fig. 1). At E8.5, when $Fz2^{-/-};Fz7^{-/-}$ embryos are only modestly smaller than control littermates, they exhibit a strikingly rotund morphology with a length:width ratio of ~2, as compared with the control ratio of ~3.5 (Fig. 1A,B,E). Over the ensuing day, $Fz2^{-/-};Fz7^{-/-}$ embryos fail to close the neural tube, develop left-right heart asymmetry, or complete tail turning (Fig. 1C,D,F-M). The abrupt growth arrest of $Fz2^{-/-};Fz7^{-/-}$ embryos might be caused, at least in part, by a failure of normal vascular development. At E9.5, the $Fz2^{-/-};Fz7^{-/-}$ embryo vasculature is underdeveloped and the yolk sac has failed to generate an organized vascular plexus, and by E10.5 the yolk sac vasculature is engorged with blood (Fig. 2). This last observation implies that hematopoiesis is not substantially affected in $Fz2^{-/-};Fz7^{-/-}$ embryos.

The morphology of $Fz2^{-/-};Fz7^{-/-}$ embryos at E8.5 suggests a severe defect in convergent extension, a process that has been associated with PCP signaling in *Xenopus*, zebrafish and mice (Goodrich and Strutt, 2011; Gray et al., 2011). Interestingly, morpholino oligonucleotide knockdowns of zebrafish *fz2* and *Xenopus Fz7* are also associated with convergent extension defects (Sumanas and Ekker, 2001; Sumanas et al., 2001). Current evidence suggests that PCP signaling controls the cytoskeleton with little or no effect on gene expression (Goodrich and Strutt, 2011; Gray et al., 2011). Microarray hybridization of RNA from $Fz7^{-/-}$ control versus $Fz2^{-/-};Fz7^{-/-}$ embryos at E8.5 shows fewer than ten transcripts with abundance changes greater than 2-fold and $P<0.05$ (supplementary material Fig. S3). Moreover, a separate analysis of 25 genes known to be induced by canonical Wnt signaling in mammals, of which 19 have been characterized as direct targets of LEF/TCF/β-catenin, showed no evidence for a decrease in canonical Wnt signaling in $Fz2^{-/-};Fz7^{-/-}$ embryos (supplementary material Fig. S4 and Table S1). The changes in transcript abundance cluster near to zero on the $\log_2$ plot, and, to the extent that those values deviate from zero, there is an accompanying increase in the *P*-value to a level that is statistically insignificant. Stated equivalently, there is no statistically significant evidence for the hypothesis of a change in transcript abundance compared with the null hypothesis of no change in abundance. These data are consistent with the idea that the morphological defect in E8.5 $Fz2^{-/-};Fz7^{-/-}$ embryos reflects a disruption of PCP signaling, which may involve few or no changes in gene expression.

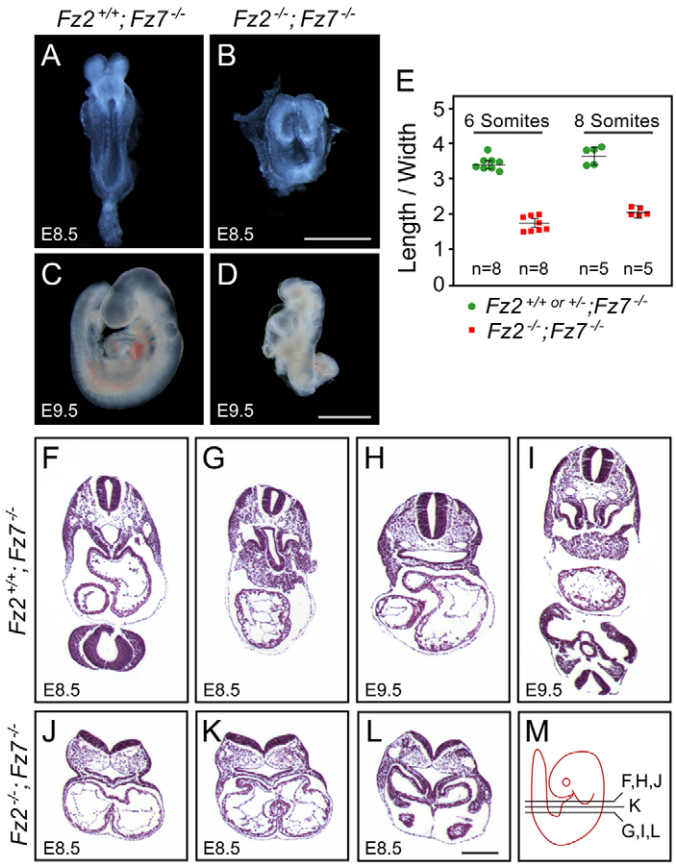

Fig. 1. $Fz2^{-/-};Fz7^{-/-}$ embryos exhibit a severe defect in convergent extension and die at ~E10.5. (**A-D**) $Fz2^{+/+};Fz7^{-/-}$ mouse embryos are indistinguishable from wild type at all stages. $Fz2^{-/-};Fz7^{-/-}$ embryos arrest growth at ~E8.5; at E9.5 they fail to turn but are still alive as judged by the presence of a heartbeat. Unstained specimens are shown. (**E**) Quantification of convergent extension, as determined by the embryo length:width ratio, among $Fz2^{-/-};Fz7^{-/-}$ and littermate control ($Fz2^{+/-};Fz7^{-/-}$ or $Fz2^{+/+};Fz7^{-/-}$) embryos at ~E8.5. Error bars indicate s.e.m. (**F-M**) H&E-stained transverse sections (as indicated in M) of the thorax from control $Fz2^{+/+};Fz7^{-/-}$ embryos at E8.5 and E9.5 and $Fz2^{-/-};Fz7^{-/-}$ embryos at E8.5. At E8.5, the $Fz2^{-/-};Fz7^{-/-}$ embryo has an open neural tube and a symmetric heart, whereas the control has a closed neural tube and exhibits left-right heart asymmetry. Scale bars: 1 mm in A-D; 200 μm in F-L.

Genetic interactions between *Fz2*, *Fz7* and *Vangl2*, *Dvl3* and Wnt genes

To broadly explore the possibility that Fz2 and Fz7 interact genetically with PCP and/or canonical Wnt signaling components,

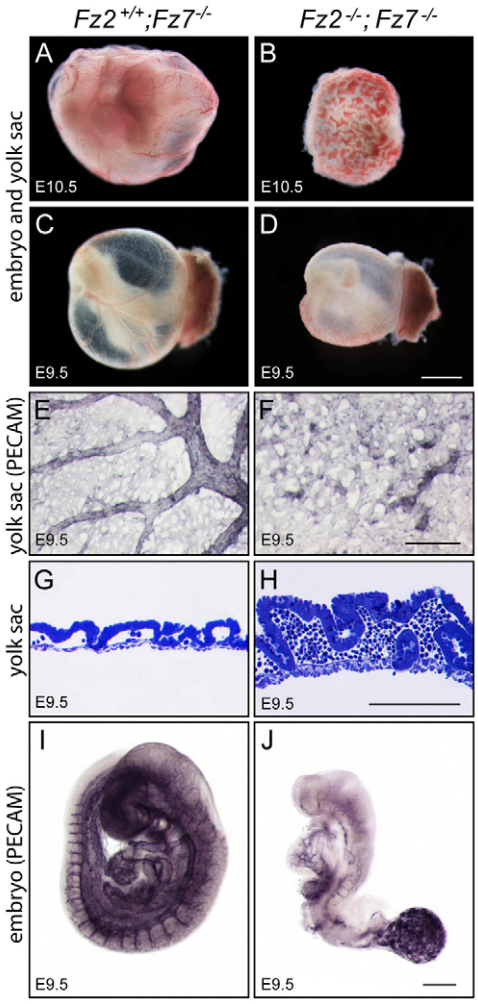

Fig. 2. Vascular defects in *Fz2*$^{-/-}$;*Fz7*$^{-/-}$ embryos. (**A-D**) *Fz2*$^{-/-}$;*Fz7*$^{-/-}$ mouse embryos are still alive at E10.5 as judged by the presence of a heartbeat, but the yolk sac shows extensive pooling of blood. Unstained specimens are shown. (**E-H**) *Fz2*$^{-/-}$;*Fz7*$^{-/-}$ yolk sac vasculature fails to differentiate into well-organized larger and smaller vessels (compare E and F; Pecam 1 immunostaining). Pooling of red blood cells in the dense capillary network is seen in transverse section (compare G and H; Toluidine Blue staining). (**I,J**) The *Fz2*$^{-/-}$;*Fz7*$^{-/-}$ embryo vasculature remains rudimentary at E9.5. Scale bars: 1 mm in A-D; 500 μm in E,F,I,J; 100 μm in G,H.

we determined the frequencies of anatomical anomalies in crosses with each of the following: *Vangl*^{Lp} [*Lp* is a semi-dominant allele (Strong and Hollander, 1949; Song, H. et al., 2010; Yin et al., 2012)], a null allele of dishevelled 3 [*Dvl3*; one of three highly homologous and partially redundant cytosolic signaling proteins involved in both canonical and PCP signaling (Etheridge et al., 2008)], and null alleles of *Wnt3a*, *Wnt5a* and *Wnt11*. *Wnt3a* was chosen for these experiments because there is strong in vivo evidence that it acts via the canonical pathway in the early embryo (Galceran et al., 2001; Nakaya et al., 2005). *Wnt5a* was chosen because it has been implicated in PCP signaling in the inner ear and is required for cardiac outflow tract development, trunk elongation and tail development (Yamaguchi et al., 1999; Qian et al., 2007; Schleiffarth et al., 2007). In cell culture, Wnt5a has been reported to act via Fz2 as well as ROR receptors and to either activate or inhibit canonical signaling depending on the receptors present (Oishi et al., 2003; Mikels and Nusse, 2006; Sato et al., 2010; Ho et al., 2012). *Wnt11* was chosen because it appears to act via a non-canonical pathway in collaboration with *Fz7* during convergent extension in zebrafish and *Xenopus* and during cardiac development in *Xenopus* (Heisenberg et al., 2000; Pandur et al., 2002; Kim et al., 2008).

Among the many combinations of genotypes examined with one or more null alleles of *Fz2* and/or *Fz7* in combination with mutant alleles of *Vangl2*, *Dvl3*, *Wnt3a*, *Wnt5a* or *Wnt11*, the most informative were the combinations with *Fz2*$^{+/-}$;*Fz7*$^{-/-}$ (Fig. 3). *Fz2*$^{+/-}$;*Fz7*$^{-/-}$ embryos appear to be at threshold for cardiac defects – in particular VSD, or less commonly VSD in combination with double-outlet right ventricle (DORV). These embryos also appear to be near threshold for palate closure defects. Cardiac defects were analyzed from Hematoxylin and Eosin (H&E) stained transverse paraffin sections obtained at late gestation (E15-18; Fig. 3A). The presence of a single *Vangl2*^{Lp} allele had little or no effect on the frequency of cardiac defects on a *Fz2*$^{+/-}$;*Fz7*$^{-/-}$ background: 37% of *Fz2*$^{+/-}$;*Fz7*$^{-/-}$;*Vangl2*^{Lp} embryos (*n*=18) were affected compared with 50% of *Fz2*$^{+/-}$;*Fz7*$^{-/-}$ embryos (*n*=22; *P*=0.537). A single *Vangl2*^{Lp} allele produced a modestly elevated frequency of cardiac defects on a *Fz7*$^{-/-}$ background: 35% of *Fz7*$^{-/-}$;*Vangl2*^{Lp} embryos were affected (*n*=20) compared with 14% for *Fz7*$^{-/-}$ (*n*=14; *P*=0.250), and, more significantly, a 50% frequency of cardiac defects was observed for *Fz2*$^{+/-}$;*Vangl2*^{Lp} embryos (*n*=6) compared with 0% for *Vangl2*^{Lp} (*n*=8; *P*=0.055) and 0% for *Fz2*$^{-/-}$ [*n*=11; reported in Yu et al. (Yu et al., 2010); *P*=0.029] embryos.

Loss of one allele of *Dvl3* increased the frequency of cardiac defects from 14% for *Fz7*$^{-/-}$ embryos (*n*=14) to 50% for *Fz7*$^{-/-}$;*Dvl3*$^{+/-}$ embryos (*n*=14; *P*=0.103) and from 50% for *Fz2*$^{+/-}$;*Fz7*$^{-/-}$ embryos (*n*=22) to 83% for *Fz2*$^{+/-}$;*Fz7*$^{-/-}$;*Dvl3*$^{+/-}$ embryos (*n*=12; *P*=0.075). *Dvl3*$^{+/-}$ embryos did not exhibit cardiac defects (*n*=5). Consistent with the high penetrance of cardiac defects observed by Etheridge et al. (Etheridge et al., 2008) in *Dvl3*$^{-/-}$ embryos, we observed three out of three *Fz7*$^{-/-}$;*Dvl3*$^{-/-}$ embryos with cardiac defects.

Loss of a single allele of *Wnt3a* or *Wnt11* similarly increased the frequency of cardiac defects. For *Wnt3a*, the increase was from 14% for *Fz7*$^{-/-}$ embryos (*n*=14) to 37% for *Fz7*$^{-/-}$;*Wnt3a*$^{+/-}$ embryos (*n*=16; *P*=0.226), and from 50% for *Fz2*$^{+/-}$;*Fz7*$^{-/-}$ embryos (*n*=22) to 92% for *Fz2*$^{+/-}$;*Fz7*$^{-/-}$;*Wnt3a*$^{+/-}$ embryos (*n*=12; *P*=0.024). With loss of one *Wnt11* allele, no cardiac defects were seen on *Fz7*$^{+/-}$ or *Fz7*$^{-/-}$ backgrounds, but 100% of *Fz2*$^{+/-}$;*Fz7*$^{-/-}$;*Wnt11*$^{+/-}$ embryos had cardiac defects (*n*=10) compared with 50% of *Fz2*$^{+/-}$;*Fz7*$^{-/-}$ embryos (*n*=22; *P*=0.006).

In a large number of crosses between *Fz2*$^{+/-}$;*Fz7*$^{-/-}$ parents, we did not see palate closure defects in *Fz7*$^{-/-}$ or *Fz2*$^{+/-}$;*Fz7*$^{-/-}$ embryos (*n*>50 each; Fig. 3B). Similarly, the presence of one or two *Vangl2*^{Lp} alleles on a wild-type background did not produce palate closure defects (*n*=20 for *Vangl2*$^{Lp/+}$ and *n*=10 for *Vangl2*$^{Lp/Lp}$ embryos). However, the presence of a single *Vangl2*^{Lp} allele produced a higher frequency of cleft palate in combination with *Fz2*$^{+/-}$;*Fz7*$^{-/-}$ (53% of *Fz2*$^{+/-}$;*Fz7*$^{-/-}$;*Vangl2*$^{Lp/+}$ embryos affected; *n*=17) compared with *Fz2*$^{+/-}$;*Fz7*$^{-/-}$ controls from the same set of crosses (15% affected; *n*=13; *P*=0.057). The occurrence of palate closure defects among *Fz2*$^{+/-}$;*Fz7*$^{-/-}$ littermate controls in this last set of crosses suggests that the *Fz2*$^{+/-}$;*Fz7*$^{-/-}$ genotype is very close to threshold for palate closure defects. This last observation suggests that non-genetic variation and/or differences in genetic background account, at least in part, for the palate closure defects seen in 4% of *Fz7*$^{-/-}$;*Vangl2*$^{Lp/+}$ embryos (*n*=25), 14% of *Fz2*$^{+/-}$;*Fz7*$^{-/-}$;*Wnt3a*$^{+/-}$ embryos (*n*=14) and 11% of *Fz2*$^{+/-}$;*Fz7*$^{-/-}$;*Wnt11*$^{+/-}$ embryos (*n*=9).

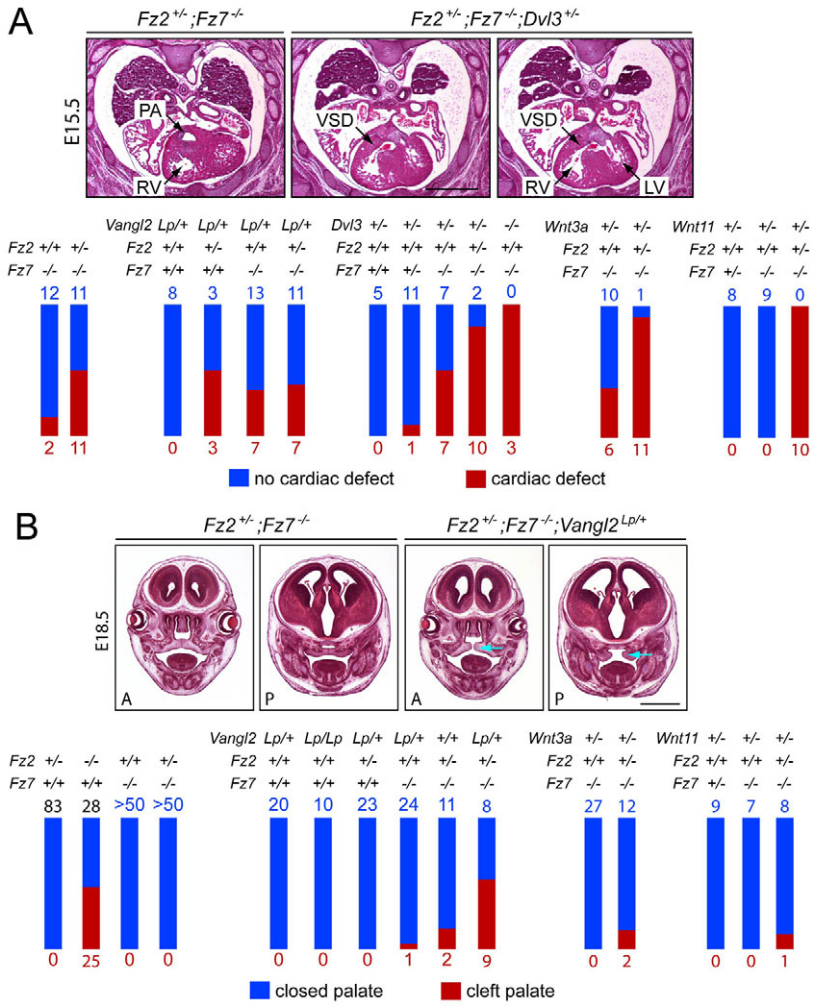

Fig. 3. Tests for genetic interactions between *Fz2*, *Fz7* and *Vangl2*, *Dvl3*, *Wnt3a* and *Wnt11*. (**A**) (Top) H&E-stained transverse paraffin sections showing cardiac defects in E15-18 mouse embryos. The vast majority were ventricular septal defects (VSDs), as seen upon comparing the normal cardiac anatomy of a $Fz2^{+/-};Fz7^{-/-}$ heart (left) with a pair of sections from a $Fz2^{+/-};Fz7^{-/-};Dvl3^{+/-}$ heart (right). PA, pulmonary artery; LV, left ventricle; RV, right ventricle. (Bottom) Summary of the numbers of embryos with the indicated genotypes and cardiac phenotypes. Each set of crosses is represented as a separate cluster of red and blue bars, with blue numbers and bars indicating embryos with no cardiac defect, and red numbers and bars indicating embryos with cardiac defects. Bar heights are normalized to the total number of embryos of the indicated genotype. (**B**) (Top) Palate closure defects in E18.5 embryos, as seen upon comparing the normal palate anatomy at anterior (A) and posterior (P) sites in an E18.5 $Fz2^{+/-};Fz7^{-/-}$ head (left pair of panels) with the cleft palate (blue arrows) of an E18.5 $Fz2^{+/-};Fz7^{-/-};Vangl2^{Lp/+}$ head (right pair of panels). Most palates were scored intact after removing the lower jaw. Bottom, summary of genotypes and palate phenotypes as described for A. Scale bars: 1 mm.

$Wnt5a^{+/-}$ mice have no apparent phenotype, but $Wnt5a^{+/-};Fz7^{-/-}$ mice show an accentuated tail truncation phenotype relative to $Fz7^{-/-}$ mice (Fig. 4A,B). With the additional loss of one copy of *Fz2*, no embryos survive beyond E11. $Fz2^{+/-};Fz7^{-/-};Wnt5a^{+/-}$ embryos arrest growth starting at ~E9.5 (Fig. 4C); the mechanism of the arrest has not been investigated.

In summary, $Fz7^{-/-}$ mice exhibit tail truncation and kinking with full penetrance and cardiac defects with low penetrance; $Fz2^{-/-}$ mice exhibit cleft palate with ~50% penetrance; $Fz2^{+/-};Fz7^{-/-}$ mice exhibit cardiac defects with ~50% penetrance and cleft palate with low penetrance; and $Fz2^{-/-};Fz7^{-/-}$ mice exhibit convergent extension defects and mid-gestational lethality with 100% penetrance. When *Fz2* and/or *Fz7* mutations are combined with mutations in one or both copies of *Vangl2*, *Dvl3*, *Wnt3a*, *Wnt5a* or *Wnt11*, increased frequencies of cardiac phenotypes are observed with *Dvl3*, *Wnt3a* and *Wnt11*; an increased frequency of palate closure defects is observed with *Vangl2*; and enhanced tail shortening and early lethality are observed with *Wnt5a*.

Cell culture assay of Frizzled signaling potential: canonical signaling

The genetic interactions described above that link *Fz2* and *Fz7* to *Vangl2*, *Dvl3*, *Wnt3a*, *Wnt5a* and *Wnt11* imply a convergence in the actions of these signaling components, but the data do not define how direct or indirect that convergence is. At one extreme, a reduction in Wnt ligand level could synergize with a reduction in Frizzled receptor level because the two components act directly as a ligand-receptor pair. However, there are many possibilities that are less direct. For example, the ligand and receptor could act through the same signaling pathway but via distinct cell surface complexes, or through different signaling pathways that later converge via their effects on some general behavior such as cell motility. It is also possible that the ligand and receptor could act on different cells and/or at different times but converge on the same biological process. For example, one component might act in one group of cells to facilitate their migration, whereas the other component might act in a second group of cells that serve as guideposts or substrates for that migration. The same ambiguity regarding the mechanism also applies to genetic interaction between receptors (Frizzled) and non-ligand signaling components (Vangl2 and Dvl3).

As one approach to constraining the mechanisms that might explain the *Fz2* and *Fz7* phenotypes and their genetic interactions, as well as to more generally assess the signaling capacities of Frizzled receptors, we have tested the activities of each mouse Frizzled protein in two assays that currently represent the best cell culture correlates of canonical and PCP signaling capacity, as described below.

For canonical signaling, we transfected cDNAs encoding each of the ten mouse Frizzleds and each of the 19 mouse Wnts in all pairwise combinations into a HEK293 cell line that responds to β-catenin stabilization and LEF/TCF activation by expression of a

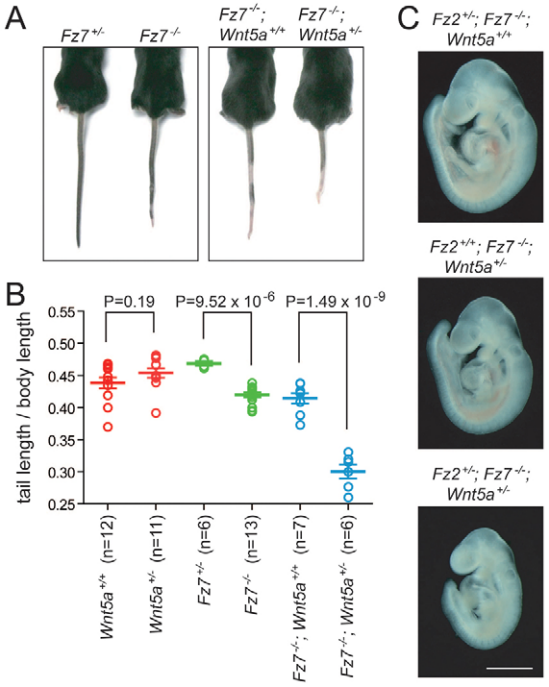

Fig. 4. *Wnt5a*$^{+/-}$ in combination with *Fz7*$^{-/-}$ enhances the short tail phenotype and in combination with *Fz2*$^{+/-}$;*Fz7*$^{-/-}$ causes mid-gestational lethality. (**A**,**B**) The only anatomical phenotype evident in *Fz7*$^{-/-}$ mice is a ~10% decrease in tail length and a small kink at the end of the tail. The scatter plot shows tail length divided by body length, measured from the nose to the base of the tail, at 4 weeks of age. *Wnt5a*$^{+/-}$ mice show no tail phenotype, but *Wn5a*$^{+/-}$ enhances the *Fz7*$^{-/-}$ tail shortening phenotype. Error bars indicate s.e.m. (**C**) E9.5 littermates illustrate the lethal growth retardation in *Fz2*$^{+/-}$;*Fz7*$^{-/-}$;*Wnt5a*$^{+/-}$ embryos. *Fz2*$^{+/-}$;*Fz7*$^{-/-}$;*Wnt5a*$^{+/+}$ and *Fz2*$^{+/+}$;*Fz7*$^{-/-}$;*Wnt5a*$^{+/+}$ embryos are unaffected at this age. Unstained specimens are shown. Scale bar: 1 mm.

firefly luciferase reporter [Super Top-Flash (STF) cells (Xu et al., 2004)]. Fig. 5 shows the results of three averaged experiments for each of the 190 Wnt-Frizzled combinations, as well as individual transfections of the 19 Wnts and ten Frizzleds. All transfections included the canonical Wnt signaling co-receptor Lrp5, and the resulting firefly luciferase values were normalized to a cotransfected *Renilla* luciferase control.

The heat maps in Fig. 5A show four representations of the same luciferase data sets (supplementary material Table S2). Each set of panels shows the individual Wnt+Lrp5 luciferase levels (left column), the individual Fz+Lrp5 luciferase levels (top row), and the 190 pairwise combinations of Wnt+Fz+Lrp5 (10×19 rectangle). Each of these three data sets have been independently color-coded with minimal and maximal values represented by fully saturated yellow and blue, respectively. Strikingly, transfection of Wnt1+Lrp5 produces a high level of luciferase activity, suggesting that STF cells might express a receptor for Wnt1. Similarly, transfection of Fz9+Lrp5 produces a high level of luciferase activity, suggesting that Fz9 can signal in a ligand-independent manner or that an Fz9 ligand might be either produced by STF cells or present in bovine serum. For the two sets of panels on the right of Fig. 5A, the individual Wnt+Fz+Lrp5 values have been corrected to show the fold change relative to the level of canonical signaling conferred by the individual Wnt+Lrp5 and Fz+Lrp5 samples. Fig. 5A also displays both linear (top) and $\log_2$ transformed (bottom) versions of the data sets; the $\log_2$ version reveals more subtle differences in signal strength. Fig. 5B shows an unsupervised hierarchical clustering of Wnts and Frizzleds based on signaling specificity and amplitude.

Several patterns emerge from these data. First, among the Frizzleds, Fz3 and Fz6 show the weakest signaling in combination with nearly all Wnts, the single exception being the combination of Wnt5b and Fz6. The low level of canonical signaling exhibited by Fz3 and Fz6 is consistent with the PCP-like phenotype of *Fz6*$^{-/-}$ (aberrant hair follicle orientation) and *Fz3*$^{-/-}$;*Fz6*$^{-/-}$ (aberrant inner ear sensory hair orientation) mice and the high sequence homology between Fz3 and Fz6 (supplementary material Fig. S2). Second, several Wnts (e.g. Wnt2, Wnt3, Wnt3a and Wnt7b) activate multiple Frizzleds, and several Frizzleds (e.g. Fz1, Fz2, Fz4, Fz5, Fz7 and Fz8) are activated by multiple Wnts. Third, Frizzleds with a high degree of amino acid sequence identity show similar patterns of Wnt activation. Thus, Fz1, Fz2 and Fz7 form one subgroup, Fz5 and Fz8 form a second subgroup, and Fz3 and Fz6 form a third subgroup.

In extrapolating these luciferase data to the in vivo situation, we note that there are a number of uncertainties. First, the efficiencies with which different Wnts and Frizzleds are correctly folded, processed and transported in STF cells are unknown. In this regard, we note that C-terminal epitope-tagged versions of all ten Frizzleds accumulate in transfected HEK293 cells (the STF parent line) to levels that are readily detected by immunostaining, and that an examination of the cell surface localization of the two Frizzleds that exhibit the weakest canonical signaling (Fz3 and Fz6) by immunostaining of living cells for an extracellular epitope tag reveals readily detectable signals (supplementary material Fig. S5). Second, differential effects of co-receptors (Lrp5 versus Lrp6) or chaperones (such as Tspan12) have not been tested. Third, differential effects of serum-derived components have not been tested. Fourth, the STF assay does not take into account the in vivo levels of ligands, receptors or intra- and extracellular modulators of canonical Wnt signaling. Finally, the biological significance of a particular level of canonical signaling is difficult to predict – a low level of signaling, could, in the appropriate context, have a large biological effect. Despite these caveats, these data represent the first comprehensive analysis of Wnt-Frizzled signaling and they are a useful starting point for assessing ligand-receptor relationships in this system.

Cell culture assay of Frizzled signaling potential: PCP signaling

At present, there is no cell culture system that reproduces PCP signaling. However, in the *Drosophila* wing disc and in the mammalian inner ear and skin, Frizzleds are arrayed on one side of each epithelial cell, Vang/Vangl proteins are arrayed on the opposite side, and Fmi/Stan/Celsr proteins are present on both sides where they appear to mediate homophilic adhesion between neighboring cells via their cadherin repeats (Goodrich and Strutt, 2011; Gray et al., 2011). This distinctive localization of a subset of core PCP proteins in epithelial cells suggests that the assembly of asymmetric cell surface complexes could serve as an assay to predict which Frizzleds have the capacity to participate in PCP signaling. Importantly, a rudimentary version of these asymmetric complexes has recently been observed in mouse keratinocytes transfected with *Celsr1*, *Fz6* and *Vangl2* (Devenport and Fuchs, 2008).

To assess the competence of each Frizzled to co-assemble with Celsr1 in surface complexes, we transfected MDCK epithelial cells

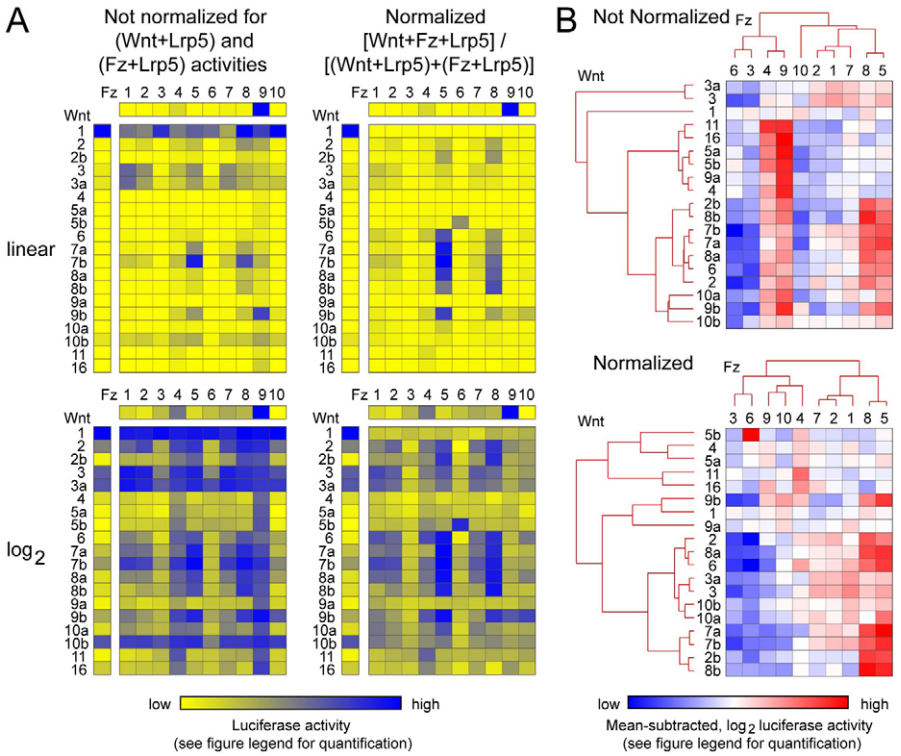

Fig. 5. Canonical Wnt signaling in STF cells induced by each of the 19 Wnts in pairwise combination with each of the ten Frizzleds. (**A**) Luciferase activity was determined following transient transfection of STF cells with: (1) each of the 19 mouse Wnts together with Lrp5 (vertical columns), (2) each of the ten mouse Frizzleds together with Lrp5 (horizontal rows), and (3) the 10×19=190 pairwise combinations of mouse Wnt and mouse Frizzled together with Lrp5 (central rectangles). Four representations of the data are shown, and all values are averages of three transfections. (Left) Not normalized, signifying that the firefly luciferase values were corrected only with respect to the *Renilla* luciferase internal control. (Right) Normalized, signifying that the firefly luciferase values were additionally normalized by calculating (Wnt+Fz+Lrp5)/[(Wnt+Lrp5)+(Fz+Lrp5)] to reveal the fold increase in luciferase activity referable specifically to the interaction between Frizzled and Wnt. Upper pair of panels, linear values; lower pair of panels, $\log_2$ values. The numerical ranges for the yellow-blue calibration bar are as follows (lowest value is pure yellow; highest value is pure blue): Wnt+Lrp5 (linear), 0.14 to 140.80; Wnt+Lrp5 ($\log_2$), –2.84 to 7.14; Fz+Lrp5 (linear), 0.26 to 16.30; Fz+Lrp5 ($\log_2$), –1.94 to 4.03; Wnt+Fz+Lrp5 (linear, not normalized), 0.19 to 170.79; Wnt+Fz+Lrp5 ($\log_2$, not normalized), –2.40 to 7.42; Wnt+Fz+Lrp5 (linear, normalized), 0.28 to 51.27; Wnt+Fz+Lrp5 ($\log_2$, normalized), –1.84 to 5.68. For each of the individual data sets – Wnt+Lrp5, Fz+Lrp5 and Wnt+Fz+Lrp5 (normalized and not normalized) – the yellow-blue calibration has been set so that the full color range corresponds to the full numerical range. Numerical values are listed in supplementary material Table S2. The luciferase activity for cells transfected with Lrp5 alone is not statistically distinguishable from the lowest values of Wnt+Lrp or Fz+Lrp combinations. (**B**) Hierarchical clustering of Wnts and Frizzleds based on luciferase activity for the not normalized and normalized data sets as defined in A (see Materials and methods for details). For the blue-white-red spectrum, the range of values for the not normalized and normalized data sets are, respectively, –4.338 to 4.2225 and –3.548 to 3.831.

with plasmids coding for: (1) Celsr1-GFP; or (2) each of the ten mouse Frizzleds (with a C-terminal epitope tag corresponding to the C-terminal ten amino acids of bovine rhodopsin, referred to as 1D4); or (3) Celsr1-GFP together with each 1D4-tagged Frizzled. Two days after transfection, we analyzed neighboring cell pairs ('doublets'). As the overall transfection efficiency was relatively low (<5%), we presume that most doublets arose from a cell division that occurred after DNA uptake. Doublets expressing Celsr1-GFP alone or in combination with a Frizzled-1D4 typically display strong accumulation of Celsr1-GFP at the junction between the adjacent cells (Fig. 6). When Frizzled-1D4 proteins are expressed without Celsr1-GFP, there is variable accumulation of Frizzled-1D4 at the plasma membrane, with Fz9-1D4 showing the most efficient accumulation. Under these conditions, most doublets do not show preferential accumulation of Frizzled-1D4 at the cell interface; two representative doublets are shown for each Frizzled-1D4 in Fig. 6. However, when Frizzled-1D4 and Celsr1-GFP are co-expressed, Fz3-1D4, Fz5-1D4 and Fz6-1D4 exhibit efficient colocalization with Celsr1-GFP at the cell interface (five representative doublets are shown for each Frizzled-1D4 + Celsr1-GFP set in Fig. 6). Fz4-1D4 occasionally (<50%) and Fz2-1D4 rarely (~10%) showed colocalization with Celsr1-GFP at the cell interface. The other Frizzled-1D4 proteins did not colocalize with Celsr1-GFP complexes (n>20 doublets). Interestingly, close inspection of MDCK cells co-expressing Fz10-1D4 and Celsr1-GFP suggests that Fz10-1D4 is actively excluded from the cell interface where Celsr1-GFP accumulates. Fz3-1D4 and Fz6-1D4 occasionally exhibited enrichment at the cell interface in the absence of Celsr1-GFP co-expression, perhaps mediated by expression of endogenous Celsr proteins in MDCK cells.

These data are consistent with the idea that Fz3 and Fz6 are largely dedicated to PCP signaling, and that Fz4 and Fz5 may be capable of PCP signaling. Although these data imply that other Frizzleds might be dedicated predominantly or exclusively to non-PCP signaling, there are two uncertainties regarding this assay that limit its interpretation. First, Celsr2 and Celsr3 have not been tested for their ability to colocalize with Frizzleds. In the case of Celsr2, we do not see an accumulation of transfected

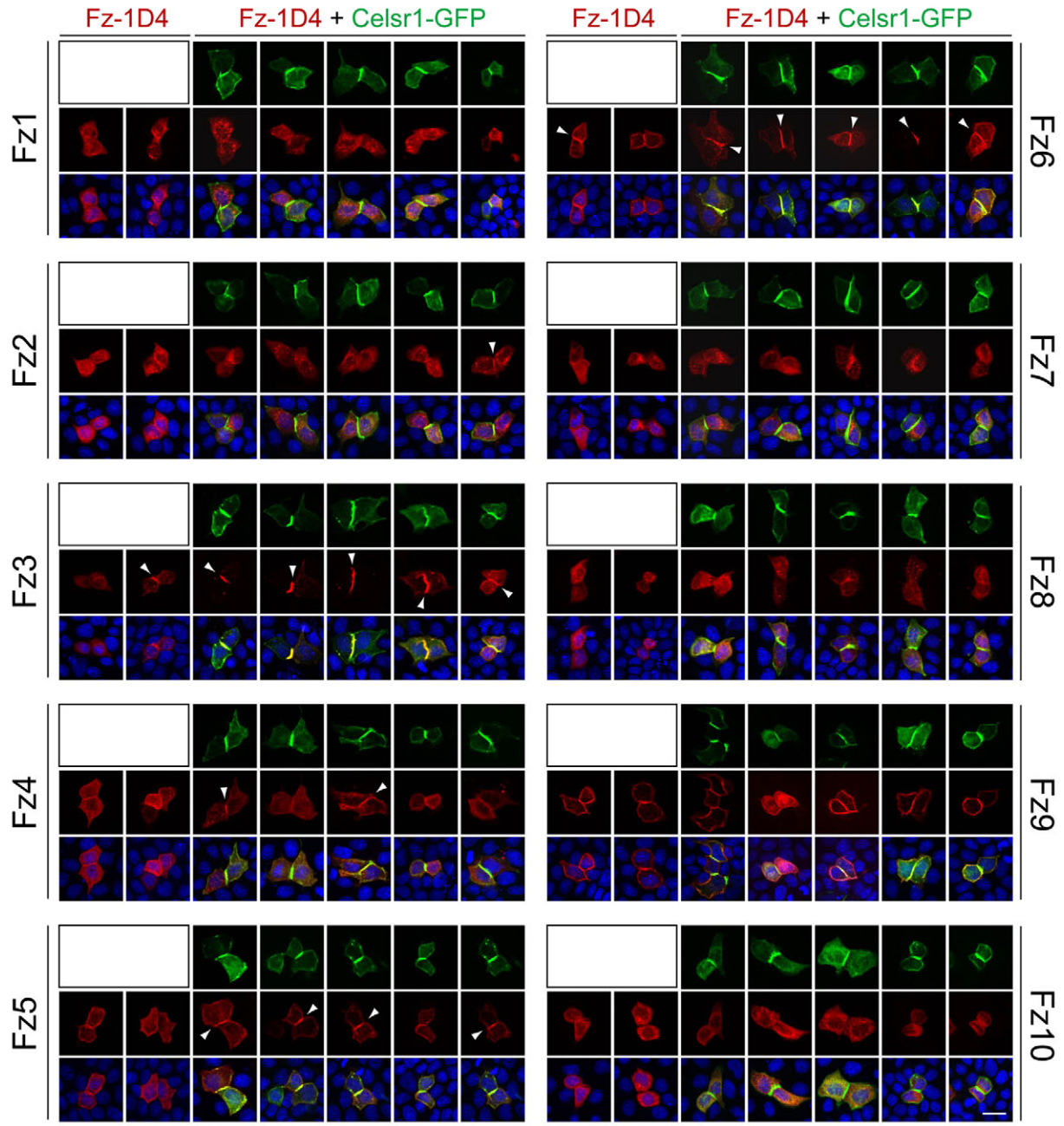

Fig. 6. Test of colocalization of each of the ten Frizzleds with Celsr1 in MDCK cells. Each of the ten mouse Frizzled-1D4 cDNAs was transiently transfected either alone or with mouse Celsr1-GFP cDNA into MDCK cells. Two days later, the subcellular distributions of the two proteins were visualized in adjacent pairs of transfected cells. For each Frizzled-1D4, two pairs of cells are shown from the transfection lacking Celsr1-GFP (first two panels in each row) followed by five pairs of cells from the transfection with Celsr1-GFP (green, top rows). Celsr1-GFP accumulates at the junction between adjacent cells, but the subcellular localization of Frizzled (red, middle rows) varies depending on the identity of the Frizzled protein. White arrowheads indicate Frizzled-1D4 co-enrichment with Celsr1-GFP at the junction between adjacent transfected cells. Bottom panel shows the merged images, with DAPI staining in blue. Scale bar: 20 μm.

Celsr2 (with a C-terminal HA tag) at cell-cell junctions, precluding a test of Celsr2-Frizzled colocalization. Second, to associate with Celsr, some Frizzleds might require additional proteins that are not present in MDCK cells or, if present, are too divergent for the canine versions to functionally interact with the expressed mouse proteins. Finally, the colocalization assay does not measure the activity of Frizzled receptors in the non-canonical regulation of Jun kinase and Rho.

DISCUSSION

The results presented here define a crucial role for *Fz2* and *Fz7* in convergent extension and cardiovascular development. They also reveal an extended web of genetic interactions between this pair of Frizzleds and a diverse set of signaling proteins involved in canonical and non-canonical signaling. In the broader context of the signaling capacities of Frizzled family members, this study also presents the first comprehensive survey of canonical signaling

across the entire Wnt and Frizzled families and the first survey of PCP-associated protein localization activity across the entire Frizzled family.

Fz1, Fz2 and Fz7 are closely related receptors that define one branch of the Frizzled family and exhibit partial redundancy. In cell culture assays, these Frizzleds can activate canonical signaling when cotransfected with a variety of Wnts, but unlike Fz3 and Fz6 they show little or no colocalization with Celsr1, suggesting that they might have a limited capacity for PCP signaling. How can one reconcile the apparently conflicting evidence that Fz2 and Fz7 mediate canonical Wnt signaling based on cell culture assays with the in vivo evidence for their role as mediators of non-canonical signaling based on the convergent extension phenotype and an apparent absence of transcript changes in *Fz2*$^{-/-}$;*Fz7*$^{-/-}$ E8.5 embryos? A number of explanations could potentially reconcile this apparent contradiction, as listed below.

First, the Celsr1 colocalization assay should be interpreted with caution as the ability of this assay to predict PCP signaling competence is not established. This caution applies most strongly in the case of a negative outcome, i.e. a failure to observe colocalization. By contrast, the activity of Fz2 and Fz7 in the STF assay can be taken as strong evidence for competence in canonical signaling. Thus, the data can be reconciled if, like *Drosophila* Fz, mammalian Fz2 and Fz7 can mediate both canonical and PCP signaling in vivo, with the latter required for convergent extension. Second, convergent extension might require canonical Wnt signaling, an idea supported by the observation of spina bifida in *Lrp6*$^{-/-}$ embryos (Pinson et al., 2000; Zhou et al., 2010). In this case, the data can be reconciled if Fz2 and Fz7 mediate canonical signaling in a minor population of cells, such that transcriptome changes are too small to detect against a large background of whole-embryo RNA. Alternately, the time window during which the relevant canonical signaling occurs might substantially predate the appearance of the convergent extension phenotype, in which case the microarray analysis at E8.5 might not reveal the relevant transcriptome changes. Third, Frizzled-mediated signaling pathways other than the canonical Wnt and PCP pathways could be relevant. We note that Fz7 signaling via the Wnt/calcium pathway has been implicated in tissue movements during *Xenopus* gastrulation (Winklbauer et al., 2001); an analogous role in mice could explain the convergent extension defect. Moreover, a new Frizzled signaling pathway – the Frizzled nuclear import (FNI) pathway – which involves proteolytic cleavage and nuclear translocation of the C-terminus of Frizzled receptors, has recently been described in *Drosophila* (Mathew et al., 2005; Speese et al., 2012). Whether this pathway operates in mammals is at present unknown. Finally, it is possible that, although the immediate cause of the *Fz2*$^{-/-}$;*Fz7*$^{-/-}$ convergent extension phenotype is a decrease in PCP signaling, this could occur indirectly if loss of Fz2 and Fz7 perturbs canonical or other signaling pathways that are linked to PCP by cross-regulatory interactions, such as those mediated by inversin (Lienkamp et al., 2012).

Genetic network analysis of Fz2 and Fz7 interactions

Genetic interactions are typically identified when alterations in one gene enhance or suppress the phenotype(s) caused by mutations in a second gene. When applied in an unbiased manner, the network of interactions thus defined is useful for identifying proteins that interact directly, act in the same pathway, or act in different pathways to affect the same biological process. Genetic interaction screens have been conducted on a genome-wide scale in prokaryotes, *S. cerevisiae*, *C. elegans* and *Drosophila*, either with the aid of mutagens or, more recently, with RNAi libraries (Dixon et al., 2009; Gunsalus and Rhrissorrakrai, 2011). In mice, genome-wide genetic interaction screens are prohibitively expensive, but targeted analyses of genetic interactions are useful for testing specific hypotheses.

In the present study, we observed genetic interactions between *Fz2* and *Fz7* and five canonical and/or non-canonical signaling molecules: mutations in *Dvl3*, *Wnt3a* or *Wnt11* enhanced the cardiac phenotype; mutation of *Vangl2* enhanced the palate closure phenotype; and mutation of *Wnt5a* enhanced the tail shortening phenotype and produced a synthetic mid-gestational lethality. If interpreted as evidence for a direct interaction between the proteins encoded by the interacting loci, this result would imply that *Fz2* and *Fz7* interact with three different Wnts and also participate in PCP signaling. We favor a more nuanced interpretation: developmental processes such as directed cell migration during palate and cardiac development (in the latter case, both long-range migration of neural crest cells and local morphogenetic movements) depend on a delicate balance of signal strength in multiple pathways, and many of these pathways are sensitive to changes of 2-fold or less in the levels of their constituent proteins. Importantly, some phenotypes with severe functional consequences, such as VSDs and palate defects, arise from a nearly correct execution of the appropriate tissue movements (Fig. 3). Apparently, small perturbations in any of a variety of signaling pathways can move the embryo from a position just beyond a critical threshold on the phenotypic landscape to a position just short of that threshold.

Redundancy among Frizzleds and other Wnt/PCP signaling components

The present work provides additional evidence that redundancy among homologous genes is widespread in vertebrate Wnt-Frizzled signaling, a phenomenon that might relate to the evolutionary expansion in the size of the gene families that encode proteins involved in these signaling pathways. For the Wnt, Frizzled, Dsh/Dvl, Vang/Vangl, Fmi/Stan/Celsr, and Arrow/Lrp families, the number of *Drosophila* and mammalian members are, respectively: seven and 19, four and ten, one and three, one and two, one and three, and one and two (supplementary material Table S1). Among mouse Frizzled genes, the functional redundancies reported thus far occur principally between closely related pairs, the one exception being *Fz4* and *Fz8* (Ye et al., 2011) (supplementary material Fig. S2). Additionally, the degree of genetic redundancy varies among pairs of Frizzled genes. The partial redundancy of *Fz3* and *Fz6* represents one end of this spectrum: defects in axon guidance are seen in *Fz3*$^{-/-}$ but not *Fz6*$^{-/-}$ mice, and defects in hair follicle orientation are seen in *Fz6*$^{-/-}$ but not *Fz3*$^{-/-}$ mice, with additional defects in neural tube closure, inner ear sensory hair cell orientation, and eyelid closure appearing in *Fz3*$^{-/-}$;*Fz6*$^{-/-}$ embryos (Wang et al., 2002; Wang et al., 2006b; Lyuksyutova et al., 2003; Guo et al., 2004). At the other end of the spectrum, *Fz1*$^{-/-}$ and *Fz8*$^{-/-}$ mice show no apparent phenotype, and the effects of gene loss are only revealed in double mutant combinations: *Fz1*$^{-/-}$;*Fz2*$^{-/-}$ embryos have fully penetrant palate closure defects compared with 50% penetrance for *Fz2*$^{-/-}$ embryos (Yu et al., 2010), *Fz4*$^{-/-}$;*Fz8*$^{-/-}$ embryos have severe renal hypoplasia compared with mild hypoplasia in *Fz4*$^{-/-}$ mice (Ye et al., 2011), and *Fz5*$^{-/-}$;*Fz8*$^{-/-}$embryos (with *Fz5* function maintained in extra-embryonic tissue) die at mid-gestation compared with the adult viability of *Fz5*$^{-/-}$ mice (Liu et al., 2012). As described here, *Fz7*$^{-/-}$

represents an intermediate case, as *Fz7*$^{-/-}$ mice exhibit a mild tail phenotype and a low-penetrance VSD phenotype, whereas *Fz2*$^{-/-}$;*Fz7*$^{-/-}$ mice show a severe defect in convergent extension. A pattern of partial redundancy similarly characterizes the *Dvl1*/*Dvl2*/*Dvl3* (Wang et al., 2006c; Etheridge et al., 2008), *Vangl1*/*Vangl2* (Torban et al., 2008; Song, H. et al., 2010) and *Lrp5*/*Lrp6* (Kelly et al., 2004; Joeng et al., 2011) gene families.

It is also striking that many combinations of mutations involving homologous genes implicated in Frizzled signaling show dosage effects, such that in comparing the progressive loss of two, three or four alleles, the phenotypes become more penetrant, more severe and/or novel. Three examples illustrate this pattern: (1) the increase in severity of renal hypoplasia in *Fz4*$^{-/-}$ versus *Fz4*$^{-/-}$;*Fz8*$^{+/-}$ versus *Fz4*$^{-/-}$;*Fz8*$^{-/-}$ embryos (Ye et al., 2011); (2) the earlier embryonic dysmorphology phenotypes in *Lrp6*$^{-/-}$ versus *Lrp6*$^{-/-}$;*Lrp5*$^{+/-}$ versus *Lrp6*$^{-/-}$;*Lrp5*$^{-/-}$ embryos (Kelly et al., 2004); and (3) the increase in severity of cardiac, inner ear and neural tube defects associated with loss of increasing numbers of Dvl family members (Wang et al., 2006c; Etheridge et al., 2008). In the present work, the comparison is between a ~15% penetrant cardiac phenotype in *Fz7*$^{-/-}$ embryos versus a ~50% penetrant cardiac phenotype with a dramatic decrease in viability in *Fz2*$^{+/-}$;*Fz7*$^{-/-}$ embryos versus a 100% penetrant convergent extension defect with mid-gestational lethality in *Fz2*$^{-/-}$;*Fz7*$^{-/-}$ embryos.

The widespread redundancy among canonical and non-canonical signaling components implies that these signaling systems have achieved a robustness to single-allele loss and, in many cases, to two-allele loss by expanding and diversifying the underlying gene repertoire. However, the gene dosage experiments imply that, even in cases with redundancy, the abundances of many signaling proteins are only 2- or 3-fold higher than the minimum threshold for normal function. These observations suggest the possibility of a selective disadvantage associated with a signal strength that is greater than several fold above the minimum threshold. Thus, in many developmental contexts, there might be a relatively narrow range of optimal signal strength, with either reduced or excessive signaling leading to loss of fitness. If this general idea is correct, it predicts that during the evolutionary process of gene duplication there might be a bottleneck in Darwinian fitness caused by the 2-fold excess of signal strength that would accompany the duplication of any gene that codes for a rate-limiting component. The present pattern of partial redundancy among closely related signaling genes might reflect the combined effects of selective pressure for gene duplication/diversification and for levels of gene expression that maintain signal strength within the optimal window.

Implications for common congenital anomalies in humans

In humans, defects in closing the ventricular septum, palate and neural tube are found in ~0.4%, ~0.1% and ~0.1% of live births, respectively, making these among the most common congenital anatomical anomalies (Centers for Disease Control, 1997; Dolk et al., 2010). Each of these anomalies appears to have complex genetic and environmental influences (Dixon et al., 2011; Au et al., 2010; Wessels and Willems, 2010; Grosen et al., 2011). For rare patients with neural tube defects, a connection to PCP signaling comes from the finding of *VANGL1*, *CELSR1*, *SCRIB* and *FUZ* (the latter two are homologs of the *Drosophila* PCP genes *scribbled* and *fuzzy*, respectively) sequence variants (Kibar et al., 2007; Kibar et al., 2009; Kibar et al., 2011; Seo et al., 2011; Robinson et al., 2012). For human palate closure defects, there are statistically significant associations with single-nucleotide polymorphisms in the *WNT3*, *WNT3A*, *WNT5A*, *WNT8A* and *WNT11* genes (Chiquet et al., 2008; Menezes et al., 2010; Yao et al., 2011; Mostowska et al., 2012). To our knowledge, no genetic studies have linked canonical or non-canonical signaling to human cardiac defects.

In mice, mutations in the following canonical and non-canonical signaling genes either alone or in combination lead to defects in ventricular septum (V), palate (P) and/or neural tube (N) closure: *Fz1* [V, P, N (Yu et al., 2010)]; *Fz2* [V, P, N (Yu et al., 2010) (present work)]; *Fz7* [V, P, N (present work); we include here the *Fz2*$^{-/-}$;*Fz7*$^{-/-}$ convergent extension phenotype in the neural tube category]; *Lrp6* [V, P, N (Pinson et al., 2000; Song et al., 2009; Song, L. et al., 2010; Zhou et al., 2010)]; *Dvl1*, *Dvl2* and *Dvl3* [V, N (Wang et al., 2006c; Etheridge et al., 2008)]; *Vangl1* [N (Torban et al., 2008)]; *Vangl2* [V, P, N (Henderson et al., 2001; Kibar et al., 2001; Murdoch et al., 2001) (present work)]; *Celsr1* [N (Curtin et al., 2003)]; and *Wnt5a* [N, P (He at al., 2008; Andersson et al., 2010)]. These mouse data, together with the human genetic studies described above, suggest that additional genetic variations in canonical and non-canonical signaling genes are likely to be identified in association with each of these common human anomalies.

Acknowledgements
We thank Amir Rattner, Connie Talbot, Yanshu Wang, John Williams and two anonymous referees for assistance and/or advice.

Funding
This work was supported by the Howard Hughes Medical institute. Deposited in PMC for release after 6 months.

Competing interests statement
The authors declare no competing financial interests.

Supplementary material
Supplementary material available online at
http://dev.biologists.org/lookup/suppl/doi:10.1242/dev.083352/-/DC1

References

Andersson, E. R., Bryjova, L., Biris, K., Yamaguchi, T. P., Arenas, E. and Bryja, V. (2010). Genetic interaction between Lrp6 and Wnt5a during mouse development. *Dev. Dyn.* **239**, 237-245.
Au, K. S., Ashley-Koch, A. and Northrup, H. (2010). Epidemiologic and genetic aspects of spina bifida and other neural tube defects. *Dev. Disabil. Res. Rev.* **16**, 6-15.
Centers for Disease Control (1997). Surveillance summaries and temporal trends in the incidence of birth defects – United States. *Morb. Mortal. Wkly. Rep.* **46**, 1171-1176.
Chiquet, B. T., Blanton, S. H., Burt, A., Ma, D., Stal, S., Mulliken, J. B. and Hecht, J. T. (2008). Variation in WNT genes is associated with non-syndromic cleft lip with or without cleft palate. *Hum. Mol. Genet.* **17**, 2212-2218.
Curtin, J. A., Quint, E., Tsipouri, V., Arkell, R. M., Cattanach, B., Copp, A. J., Henderson, D. J., Spurr, N., Stanier, P., Fisher, E. M. et al. (2003). Mutation of Celsr1 disrupts planar polarity of inner ear hair cells and causes severe neural tube defects in the mouse. *Curr. Biol.* **13**, 1129-1133.
Devenport, D. and Fuchs, E. (2008). Planar polarization in embryonic epidermis orchestrates global asymmetric morphogenesis of hair follicles. *Nat. Cell Biol.* **10**, 1257-1268.
Dixon, S. J., Costanzo, M., Baryshnikova, A., Andrews, B. and Boone, C. (2009). Systematic mapping of genetic interaction networks. *Annu. Rev. Genet.* **43**, 601-625.
Dixon, M. J., Marazita, M. L., Beaty, T. H. and Murray, J. C. (2011). Cleft lip and palate: understanding genetic and environmental influences. *Nat. Rev. Genet.* **12**, 167-178.
Dolk, H., Loane, M. and Garne, E. (2010). The prevalence of congenital anomalies in Europe. *Adv. Exp. Med. Biol.* **686**, 349-364.
Etheridge, S. L., Ray, S., Li, S., Hamblet, N. S., Lijam, N., Tsang, M., Greer, J., Kardos, N., Wang, J., Sussman, D. J. et al. (2008). Murine dishevelled 3 functions in redundant pathways with dishevelled 1 and 2 in normal cardiac outflow tract, cochlea, and neural tube development. *PLoS Genet.* **4**, e1000259.
Galceran, J., Hsu, S. C. and Grosschedl, R. (2001). Rescue of a Wnt mutation by an activated form of LEF-1: regulation of maintenance but not initiation of Brachyury expression. *Proc. Natl. Acad. Sci. USA* **98**, 8668-8673.

Goodrich, L. V. and Strutt, D. (2011). Principles of planar polarity in animal development. *Development* **138**, 1877-1892.
Gray, R. S., Roszko, I. and Solnica-Krezel, L. (2011). Planar cell polarity: coordinating morphogenetic cell behaviors with embryonic polarity. *Dev. Cell* **21**, 120-133.
Grosen, D., Bille, C., Petersen, I., Skytthe, A., Hjelmborg, J., Pedersen, J. K., Murray, J. C. and Christensen, K. (2011). Risk of oral clefts in twins. *Epidemiology* **22**, 313-319.
Gunsalus, K. C. and Rhrissorrakrai, K. (2011). Networks in *Caenorhabditis elegans*. *Curr. Opin. Genet. Dev.* **21**, 787-798.
Guo, N., Hawkins, C. and Nathans, J. (2004). Frizzled6 controls hair patterning in mice. *Proc. Natl. Acad. Sci. USA* **101**, 9277-9281.
He, F., Xiong, W., Yu, X., Espinoza-Lewis, R., Liu, C., Gu, S., Nishita, M., Suzuki, K., Yamada, G., Minami, Y. et al. (2008). Wnt5a regulates directional cell migration and cell proliferation via Ror2-mediated noncanonical pathway in mammalian palate development. *Development* **135**, 3871-3879.
Heisenberg, C. P., Tada, M., Rauch, G. J., Saúde, L., Concha, M. L., Geisler, R., Stemple, D. L., Smith, J. C. and Wilson, S. W. (2000). Silberblick/Wnt11 mediates convergent extension movements during zebrafish gastrulation. *Nature* **405**, 76-81.
Henderson, D. J., Conway, S. J., Greene, N. D., Gerrelli, D., Murdoch, J. N., Anderson, R. H. and Copp, A. J. (2001). Cardiovascular defects associated with abnormalities in midline development in the Loop-tail mouse mutant. *Circ. Res.* **89**, 6-12.
Ho, H. Y., Susman, M. W., Bikoff, J. B., Ryu, Y. K., Jonas, A. M., Hu, L., Kuruvilla, R. and Greenberg, M. E. (2012). Wnt5a-Ror-Dishevelled signaling constitutes a core developmental pathway that controls tissue morphogenesis. *Proc. Natl. Acad. Sci. USA* **109**, 4044-4051.
Joeng, K. S., Schumacher, C. A., Zylstra-Diegel, C. R., Long, F. and Williams, B. O. (2011). Lrp5 and Lrp6 redundantly control skeletal development in the mouse embryo. *Dev. Biol.* **359**, 222-229.
Kelly, O. G., Pinson, K. I. and Skarnes, W. C. (2004). The Wnt co-receptors Lrp5 and Lrp6 are essential for gastrulation in mice. *Development* **131**, 2803-2815.
Kibar, Z., Vogan, K. J., Groulx, N., Justice, M. J., Underhill, D. A. and Gros, P. (2001). Ltap, a mammalian homolog of Drosophila Strabismus/Van Gogh, is altered in the mouse neural tube mutant Loop-tail. *Nat. Genet.* **28**, 251-255.
Kibar, Z., Torban, E., McDearmid, J. R., Reynolds, A., Berghout, J., Mathieu, M., Kirillova, I., De Marco, P., Merello, E., Hayes, J. M. et al. (2007). Mutations in VANGL1 associated with neural-tube defects. *N. Engl. J. Med.* **356**, 1432-1437.
Kibar, Z., Bosoi, C. M., Kooistra, M., Salem, S., Finnell, R. H., De Marco, P., Merello, E., Bassuk, A. G., Capra, V. and Gros, P. (2009). Novel mutations in VANGL1 in neural tube defects. *Hum. Mutat.* **30**, E706-E715.
Kibar, Z., Salem, S., Bosoi, C. M., Pauwels, E., De Marco, P., Merello, E., Bassuk, A. G., Capra, V. and Gros, P. (2011). Contribution of VANGL2 mutations to isolated neural tube defects. *Clin. Genet.* **80**, 76-82.
Kim, G. H., Her, J. H. and Han, J. K. (2008). Ryk cooperates with Frizzled 7 to promote Wnt11-mediated endocytosis and is essential for *Xenopus laevis* convergent extension movements. *J. Cell Biol.* **182**, 1073-1082.
Lienkamp, S., Ganner, A. and Walz, G. (2012). Inversin, Wnt signaling and primary cilia. *Differentiation* **83**, S49-S55.
Liu, C., Bakeri, H., Li, T. and Swaroop, A. (2012). Regulation of retinal progenitor expansion by Frizzled receptors: implications for microphthalmia and retinal coloboma. *Hum. Mol. Genet.* **21**, 1848-1860.
Lyuksyutova, A. I., Lu, C. C., Milanesio, N., King, L. A., Guo, N., Wang, Y., Nathans, J., Tessier-Lavigne, M. and Zou, Y. (2003). Anterior-posterior guidance of commissural axons by Wnt-frizzled signaling. *Science* **302**, 1984-1988.
Mathew, D., Ataman, B., Chen, J., Zhang, Y., Cumberledge, S. and Budnik, V. (2005). Wingless signaling at synapses is through cleavage and nuclear import of receptor DFrizzled2. *Science* **310**, 1344-1347.
Menezes, R., Letra, A., Kim, A. H., Küchler, E. C., Day, A., Tannure, P. N., Gomes da Motta, L., Paiva, K. B., Granjeiro, J. M. and Vieira, A. R. (2010). Studies with Wnt genes and nonsyndromic cleft lip and palate. *Birth Defects Res. A Clin. Mol. Teratol.* **88**, 995-1000.
Mikels, A. J. and Nusse, R. (2006). Purified Wnt5a protein activates or inhibits beta-catenin-TCF signaling depending on receptor context. *PLoS Biol.* **4**, e115.
Molday, R. S. and MacKenzie, D. (1983). Monoclonal antibodies to rhodopsin: characterization, cross-reactivity, and application as structural probes. *Biochemistry* **22**, 653-660.
Mostowska, A., Hozyasz, K. K., Biedziak, B., Wojcicki, P., Lianeri, M. and Jagodzinski, P. P. (2012). Genotype and haplotype analysis of WNT genes in non-syndromic cleft lip with or without cleft palate. *Eur. J. Oral Sci.* **120**, 1-8.
Murdoch, J. N., Doudney, K., Paternotte, C., Copp, A. J. and Stanier, P. (2001). Severe neural tube defects in the loop-tail mouse result from mutation of Lpp1, a novel gene involved in floor plate specification. *Hum. Mol. Genet.* **10**, 2593-2601.
Nakaya, M. A., Biris, K., Tsukiyama, T., Jaime, S., Rawls, J. A. and Yamaguchi, T. P. (2005). Wnt3a links left-right determination with segmentation and anteroposterior axis elongation. *Development* **132**, 5425-5436.
Oishi, I., Suzuki, H., Onishi, N., Takada, R., Kani, S., Ohkawara, B., Koshida, I., Suzuki, K., Yamada, G., Schwabe, G. C. et al. (2003). The receptor tyrosine kinase Ror2 is involved in non-canonical Wnt5a/JNK signalling pathway. *Genes Cells* **8**, 645-654.
Pandur, P., Läsche, M., Eisenberg, L. M. and Kühl, M. (2002). Wnt-11 activation of a non-canonical Wnt signalling pathway is required for cardiogenesis. *Nature* **418**, 636-641.
Pinson, K. I., Brennan, J., Monkley, S., Avery, B. J. and Skarnes, W. C. (2000). An LDL-receptor-related protein mediates Wnt signalling in mice. *Nature* **407**, 535-538.
Qian, D., Jones, C., Rzadzinska, A., Mark, S., Zhang, X., Steel, K. P., Dai, X. and Chen, P. (2007). Wnt5a functions in planar cell polarity regulation in mice. *Dev. Biol.* **306**, 121-133.
Robinson, A., Escuin, S., Doudney, K., Vekemans, M., Stevenson, R. E., Greene, N. D., Copp, A. J. and Stanier, P. (2012). Mutations in the planar cell polarity genes CELSR1 and SCRIB are associated with the severe neural tube defect craniorachischisis. *Hum. Mutat.* **33**, 440-447.
Sato, A., Yamamoto, H., Sakane, H., Koyama, H. and Kikuchi, A. (2010). Wnt5a regulates distinct signalling pathways by binding to Frizzled2. *EMBO J.* **29**, 41-54.
Schleiffarth, J. R., Person, A. D., Martinsen, B. J., Sukovich, D. J., Neumann, A., Baker, C. V., Lohr, J. L., Cornfield, D. N., Ekker, S. C. and Petryk, A. (2007). Wnt5a is required for cardiac outflow tract septation in mice. *Pediatr. Res.* **61**, 386-391.
Seo, J. H., Zilber, Y., Babayeva, S., Liu, J., Kyriakopoulos, P., De Marco, P., Merello, E., Capra, V., Gros, P. and Torban, E. (2011). Mutations in the planar cell polarity gene, Fuzzy, are associated with neural tube defects in humans. *Hum. Mol. Genet.* **20**, 4324-4333.
Song, L., Li, Y., Wang, K., Wang, Y. Z., Molotkov, A., Gao, L., Zhao, T., Yamagami, T., Wang, Y., Gan, Q. et al. (2009). Lrp6-mediated canonical Wnt signaling is required for lip formation and fusion. *Development* **136**, 3161-3171.
Song, H., Hu, J., Chen, W., Elliott, G., Andre, P., Gao, B. and Yang, Y. (2010). Planar cell polarity breaks bilateral symmetry by controlling ciliary positioning. *Nature* **466**, 378-382.
Song, L., Li, Y., Wang, K. and Zhou, C. J. (2010). Cardiac neural crest and outflow tract defects in Lrp6 mutant mice. *Dev. Dyn.* **239**, 200-210.
Speese, S. D., Ashley, J., Jokhi, V., Nunnari, J., Barria, R., Li, Y., Ataman, B., Koon, A., Chang, Y. T., Li, Q. et al. (2012). Nuclear envelope budding enables large ribonucleoprotein particle export during synaptic Wnt signaling. *Cell* **149**, 832-846.
Strong, L. C. and Hollander, W. F. (1949). Hereditary loop-tail in the house mouse accompanied by imperforate vagina and with lethal craniorachischisis when homozygous. *J. Hered.* **40**, 329-334.
Sumanas, S. and Ekker, S. C. (2001). *Xenopus* frizzled-7 morphant displays defects in dorsoventral patterning and convergent extension movements during gastrulation. *Genesis* **30**, 119-122.
Sumanas, S., Kim, H. J., Hermanson, S. and Ekker, S. C. (2001). Zebrafish frizzled-2 morphant displays defects in body axis elongation. *Genesis* **30**, 114-118.
Takada, S., Stark, K. L., Shea, M. J., Vassileva, G., McMahon, J. A. and McMahon, A. P. (1994). Wnt-3a regulates somite and tailbud formation in the mouse embryo. *Genes Dev.* **8**, 174-189.
Torban, E., Patenaude, A. M., Leclerc, S., Rakowiecki, S., Gauthier, S., Andelfinger, G., Epstein, D. J. and Gros, P. (2008). Genetic interaction between members of the Vangl family causes neural tube defects in mice. *Proc. Natl. Acad. Sci. USA* **105**, 3449-3454.
van Amerongen, R. and Nusse, R. (2009). Towards an integrated view of Wnt signaling in development. *Development* **136**, 3205-3214.
Wang, Y., Thekdi, N., Smallwood, P. M., Macke, J. P. and Nathans, J. (2002). Frizzled-3 is required for the development of major fiber tracts in the rostral CNS. *J. Neurosci.* **22**, 8563-8573.
Wang, Y., Badea, T. and Nathans, J. (2006a). Order from disorder: Self-organization in mammalian hair patterning. *Proc. Natl. Acad. Sci. USA* **103**, 19800-19805.
Wang, Y., Guo, N. and Nathans, J. (2006b). The role of Frizzled3 and Frizzled6 in neural tube closure and in the planar polarity of inner-ear sensory hair cells. *J. Neurosci.* **26**, 2147-2156.
Wang, J., Hamblet, N. S., Mark, S., Dickinson, M. E., Brinkman, B. C., Segil, N., Fraser, S. E., Chen, P., Wallingford, J. B. and Wynshaw-Boris, A. (2006c). Dishevelled genes mediate a conserved mammalian PCP pathway to regulate convergent extension during neurulation. *Development* **133**, 1767-1778.
Wessels, M. W. and Willems, P. J. (2010). Genetic factors in non-syndromic congenital heart malformations. *Clin. Genet.* **78**, 103-123.
Winklbauer, R., Medina, A., Swain, R. K. and Steinbeisser, H. (2001). Frizzled-7 signalling controls tissue separation during *Xenopus* gastrulation. *Nature* **413**, 856-860.

Xu, Q., Wang, Y., Dabdoub, A., Smallwood, P. M., Williams, J., Woods, C., Kelley, M. W., Jiang, L., Tasman, W., Zhang, K. et al. (2004). Vascular development in the retina and inner ear: control by Norrin and Frizzled-4, a high-affinity ligand-receptor pair. *Cell* **116**, 883-895.

Yamaguchi, T. P., Bradley, A., McMahon, A. P. and Jones, S. (1999). A Wnt5a pathway underlies outgrowth of multiple structures in the vertebrate embryo. *Development* **126**, 1211-1223.

Yao, T., Yang, L., Li, P. Q., Wu, H., Xie, H. B., Shen, X. and Xie, X. D. (2011). Association of Wnt3A gene variants with non-syndromic cleft lip with or without cleft palate in Chinese population. *Arch. Oral Biol.* **56**, 73-78.

Ye, X., Wang, Y., Cahill, H., Yu, M., Badea, T. C., Smallwood, P. M., Peachey, N. S. and Nathans, J. (2009). Norrin, frizzled-4, and Lrp5 signaling in endothelial cells controls a genetic program for retinal vascularization. *Cell* **139**, 285-298.

Ye, X., Wang, Y., Rattner, A. and Nathans, J. (2011). Genetic mosaic analysis reveals a major role for frizzled 4 and frizzled 8 in controlling ureteric growth in the developing kidney. *Development* **138**, 1161-1172.

Yin, H., Copley, C. O., Goodrich, L. V. and Deans, M. R. (2012). Comparison of phenotypes between different vangl2 mutants demonstrates dominant effects of the Looptail mutation during hair cell development. *PLoS ONE* **7**, e31988.

Yu, H., Smallwood, P. M., Wang, Y., Vidaltamayo, R., Reed, R. and Nathans, J. (2010). Frizzled 1 and frizzled 2 genes function in palate, ventricular septum and neural tube closure: general implications for tissue fusion processes. *Development* **137**, 3707-3717.

Zhou, C. J., Wang, Y. Z., Yamagami, T., Zhao, T., Song, L. and Wang, K. (2010). Generation of Lrp6 conditional gene-targeting mouse line for modeling and dissecting multiple birth defects/congenital anomalies. *Dev. Dyn.* **239**, 318-326.

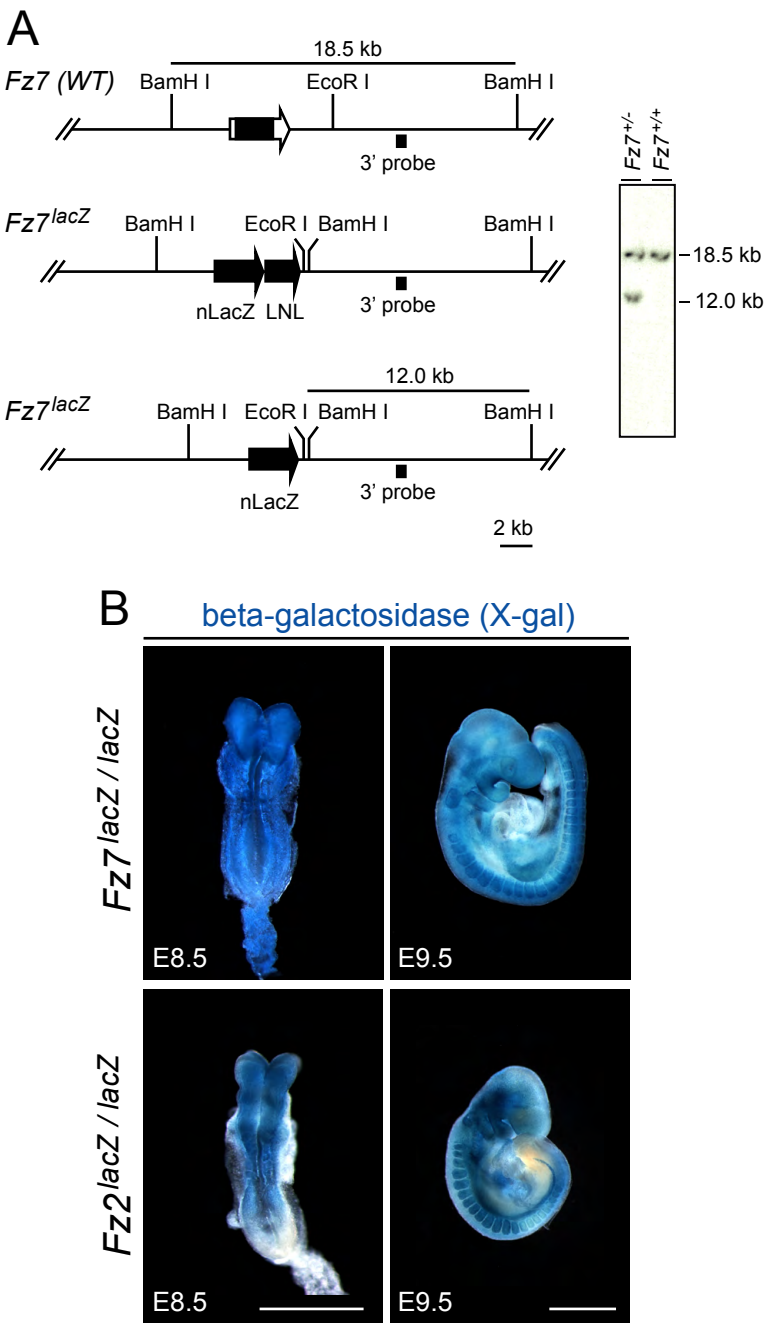

Fig. S1. *Fz7* knockout strategy and expression patterns of *Fz2*^{lacZ} and *Fz7*^{lacZ} in early embryos. (**A**) Targeted mutation of *Fz7*, with replacement of the *Fz7* coding region with a nuclear-localized *lacZ* (*nlacZ*) coding region. *LNL*, *loxP-PGK-neo-loxP* cassette, which was excised by germline Cre-mediated recombination. The 3′ Southern blot probe is indicated below the restriction maps, the 18.5 kb (native) and 12.0 kb (targeted) *Bam*HI fragments visualized by Southern blotting with this probe are indicated above the restriction maps, and a representative Southern blot is shown to the right. (**B**) X-Gal staining of *Fz7*$^{lacZ/lacZ}$ and *Fz2*$^{lacZ/lacZ}$ embryos at E8.5 (dorsal view) and E9.5 (side view) shows widespread expression of both genes in ectoderm and mesoderm. Scale bars: 1 mm.

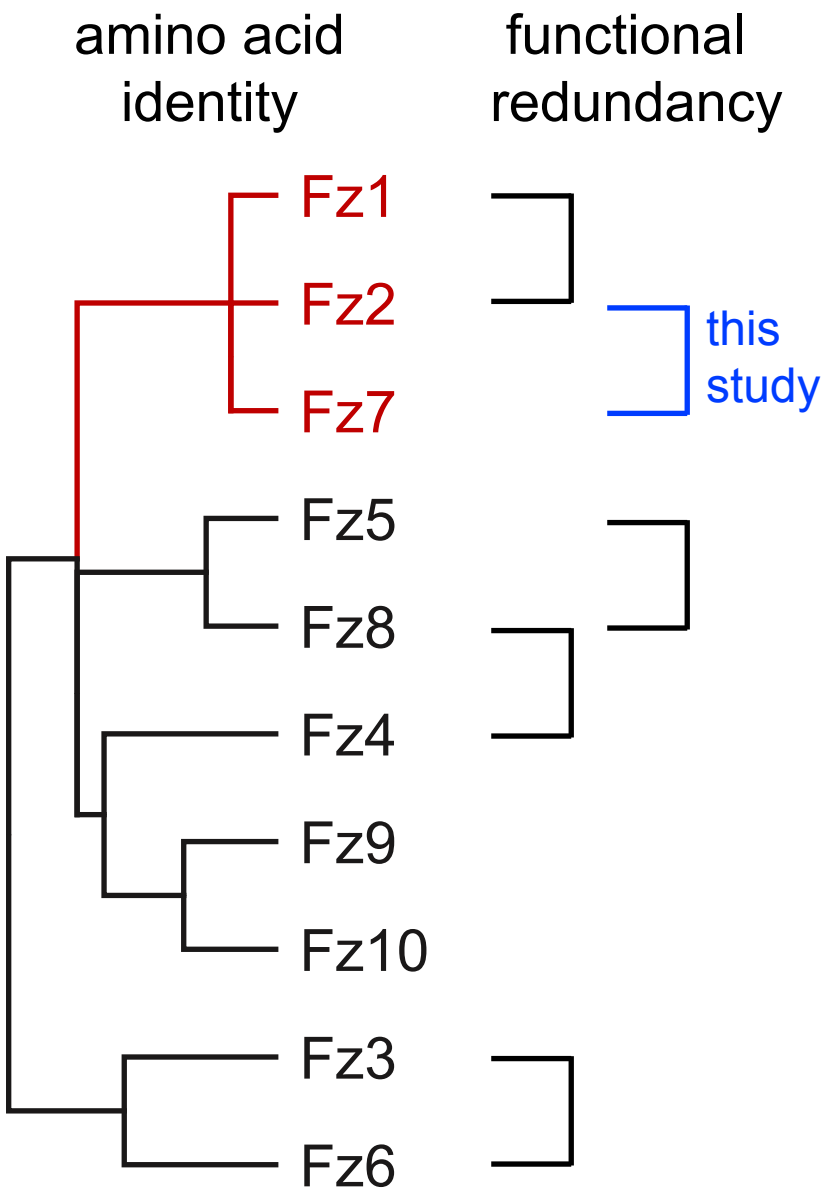

Fig. S2. Dendrogram showing amino acid sequence identity among mouse Frizzled proteins. Fz1, Fz2 and Fz7 (red) constitute a distinct branch within the Frizzled family. The dendrograms were generated from multiple sequence alignments produced by MEGA4 software. Previously described functional redundancies among Frizzled family members are indicated by the brackets and are described in the following references: *Fz1/Fz2* (Yu et al., 2010); *Fz3/Fz6* (Wang et al., 2006b); *Fz4/Fz8* (Ye et al., 2011); *Fz5/Fz8* (Liu et al., 2012). The blue bracket represents the *Fz2/Fz7* redundancy described in the present study.

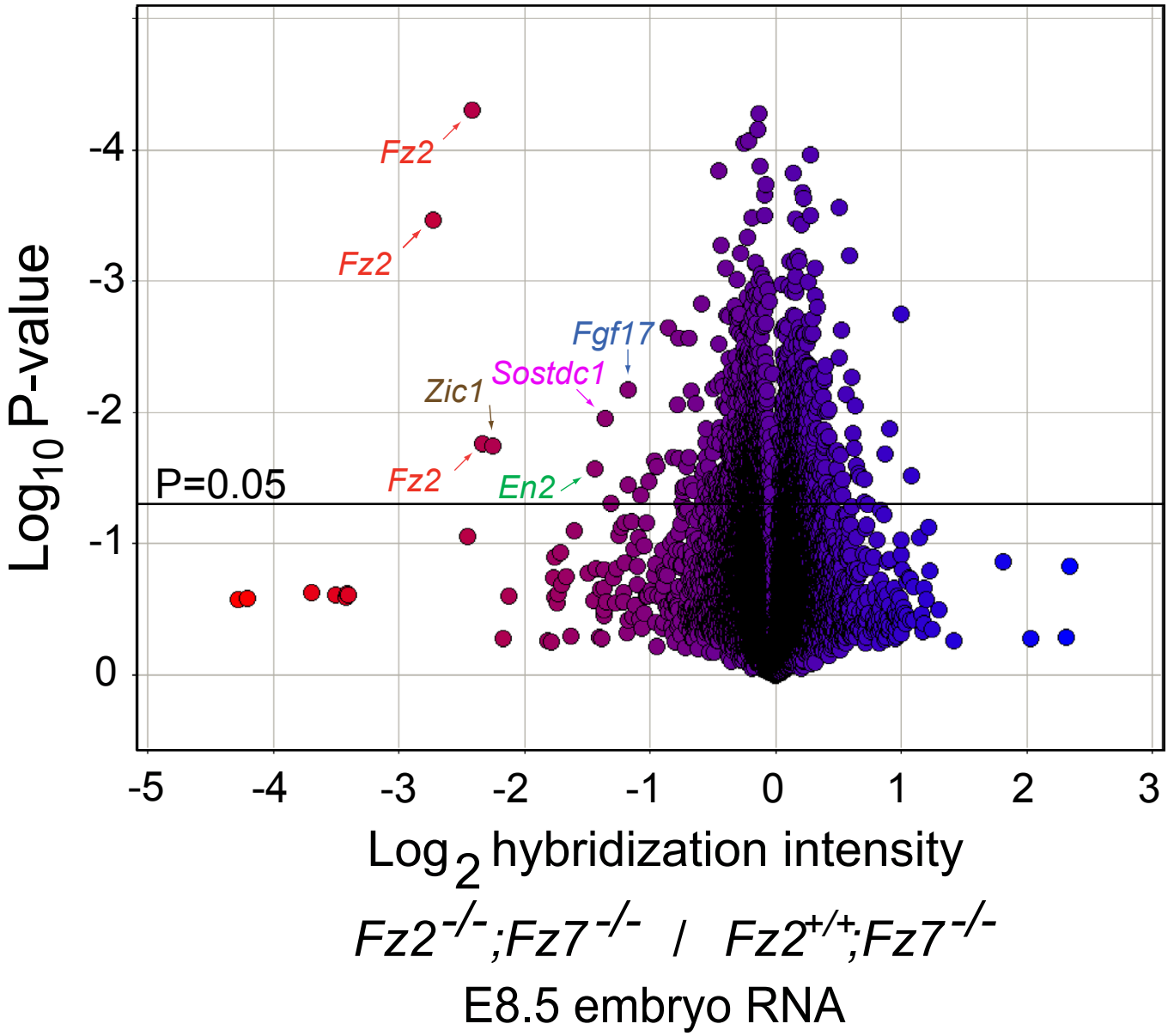

Fig. S3. Microarray hybridization comparison of E8.5 littermate *Fz2*$^{-/-}$;*Fz7*$^{-/-}$ and *Fz2*$^{+/+}$;*Fz7*$^{-/-}$ transcriptomes. Volcano plot showing the result of three biologically independent hybridizations to Affymetrix 430 2.0 microarrays, with hybridization intensity ratios plotted on a $\log_2$ scale, and *P*-values plotted on a $\log_{10}$ scale. The horizontal black line represents *P*=0.05. Each transcript is generally represented by multiple sets of oligonucleotide targets, multiple entries in the Affymetrix spreadsheet, and, therefore, multiple points on the volcano plot. The volcano plot shows the expected decrease in the abundance of *Fz2* transcripts, which are absent in *Fz2*$^{-/-}$;*Fz7*$^{-/-}$ embryos. The primary data are available at the Gene Expression Omnibus under accession number GSE37221.

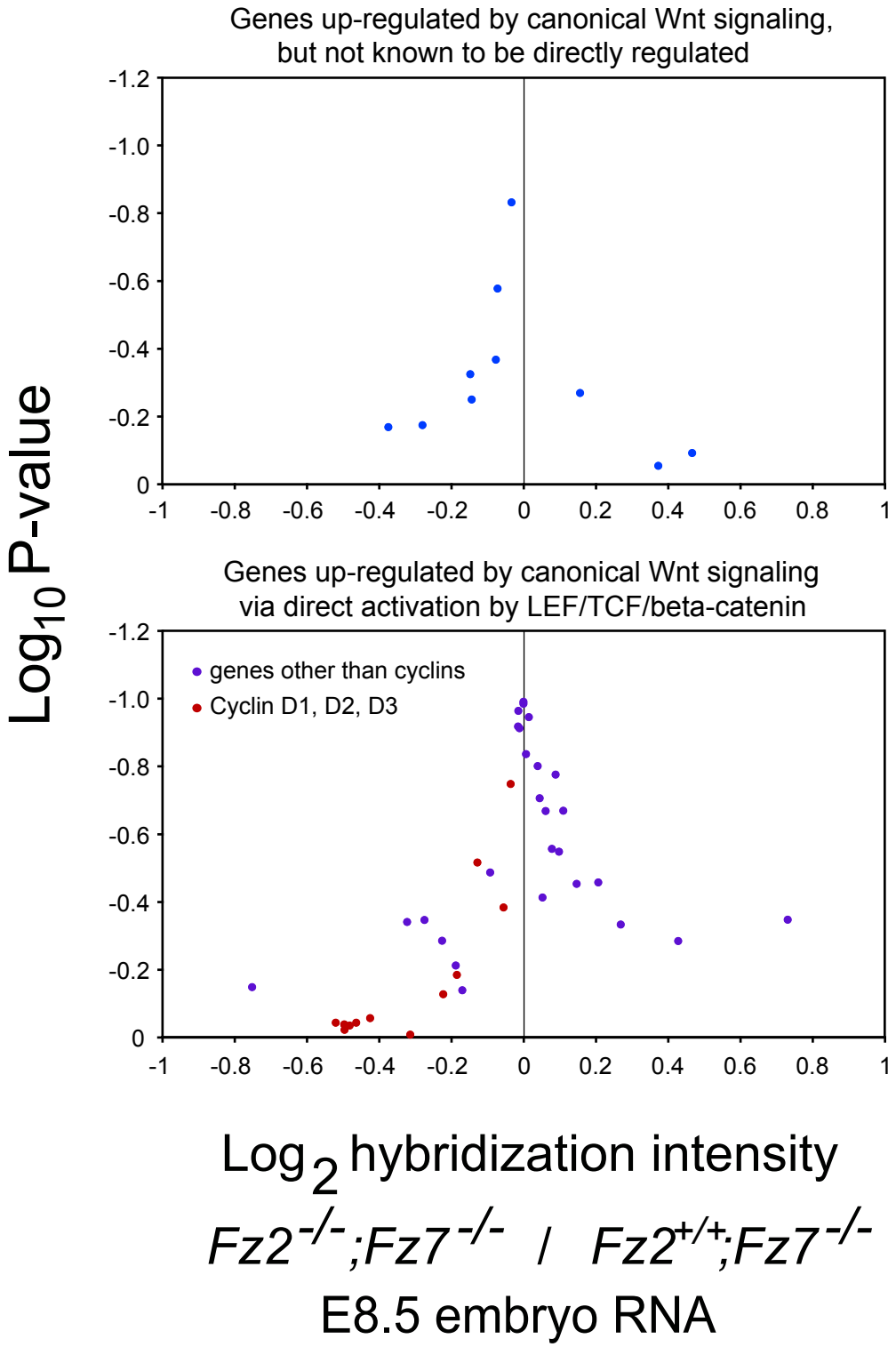

Fig. S4. Microarray hybridization comparison of E8.5 littermate *Fz2*$^{-/-}$;*Fz7*$^{-/-}$ and *Fz2*$^{+/+}$;*Fz7*$^{-/-}$ for a subset of 25 genes induced by canonical Wnt signaling. Volcano plots showing the result of three biologically independent hybridizations to Affymetrix 430 2.0 microarrays, with hybridization intensity ratios plotted on a $\log_2$ scale, and *P*-values plotted on a $\log_{10}$ scale. The 25 Wnt-responsive genes are divided into two plots for those that are (lower plot) or are not (upper plot) known to be direct targets of LEF/TCF/β-catenin signaling (see summary at http://www.stanford.edu/group/nusselab/cgi-bin/wnt/target_genes). Each transcript is generally represented by multiple sets of oligonucleotide targets, multiple entries in the Affymetrix spreadsheet, and, therefore, multiple points on the volcano plot (see Table S1). Data points corresponding to Cyclin D family members, which have the largest number of probe sets, are color-coded red.

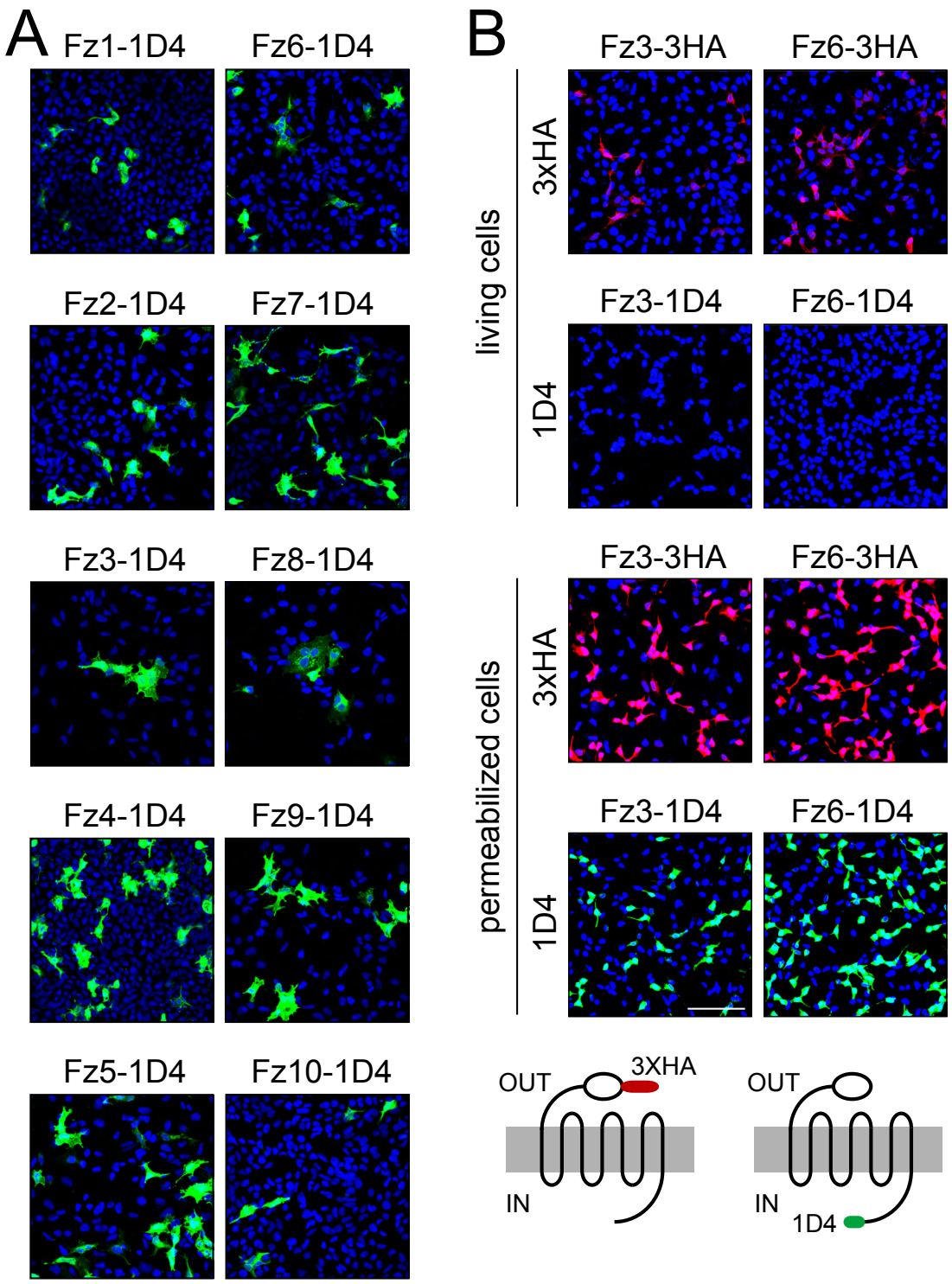

Fig. S5. Analysis of expression of Fz1-Fz10 and cell surface localization of Fz3 and Fz6 in HEK293 cells. (**A**) HEK293 cells transiently transfected with plasmids coding for 1D4 C-terminal epitope-tagged Fz1 through Fz10 were fixed, permeabilized with Triton X-100, and immunostained with mAb 1D4. Transfection and immunostaining were performed in parallel with common reagent mixes, confocal imaging was performed with identical settings, and image processing was performed with identical parameters. (**B**) HEK293 cells transiently transfected with plasmids coding for epitope-tagged Fz3 or Fz6 proteins (diagramed beneath) were incubated with primary antibodies under one of two conditions: (1) as living cells, followed by paraformaldehyde fixation or (2) following paraformaldehyde fixation and permeabilization. For all samples, secondary antibody binding was conducted under permeabilizing conditions. For each antibody, permeabilized and non-permeabilized confocal imaging was performed with identical settings. For all images, image processing was performed with identical parameters. The failure of mAb 1D4 to stain living cells is consistent with the intracellular localization of this C-terminal epitope. The lower level of 3×HA binding to living cells compared with fixed and permeabilized cells is likely to reflect a combination of the accumulation of the majority of Fz3 and Fz6 within the secretory pathway and the ~15× shorter primary antibody incubation time used for living cells compared with permeabilized cells. Scale bar: 100 μm.

Table S1. Transcript abundance changes in *Fz2*$^{-/-}$ versus *Fz2*$^{-/-}$;*Fz7*$^{-/-}$ E8.5 embryos among 25 genes known to be induced by canonical Wnt signaling

Shown are Affymetrix probe set ID and gene symbol, the average hybridization intensity changes based on three independent sets of *Fz2*$^{-/-}$ versus *Fz2*$^{-/-}$;*Fz7*$^{-/-}$ E8.5 embryos, and the *P*-value of the resulting fold change versus the null hypothesis of no change. The numbers to the left refer to the row number in the full microarray hybridization data set (GEO accession number GSE37221). The 25 genes are divided into those known to be directly regulated by canonical Wnt signaling (i.e. by LEF/TCF/beta-catenin binding to DNA target sequences) (19/25 genes, upper table) and those not known to be directly regulated (6/25 genes, lower table); Wnt induction data are summarized at http://www.stanford.edu/group/nusselab/cgi-bin/wnt/target_genes.

Genes directly upregulated by LEF/TCF/beta-catenin

Number	$\log_2$ fold change	Fold change	*P*-value	Probe set ID	Gene symbol
9249	-0.223984329	-1.167954708	0.28289708	1424942_a_at	*Myc*
17778	-0.090327432	-1.064611778	0.48436968	1433471_at	*Tcf7*
34757	0.001656169	1.001148628	0.988533869	1450461_at	*Tcf7*
5606	0.090918542	1.065048066	0.773563439	1421299_a_at	*Lef1*
39030	-0.185546083	-1.137247358	0.210292884	1454734_at	*Lef1*
7221	0.208727406	1.155668325	0.45537026	1422914_at	*Sp5*
34550	0.054642591	1.038601772	0.410765538	1450254_at	*Tert*
5648	0.046504224	1.032759424	0.703458327	1421341_at	*Axin2*
21152	-0.013186043	-1.009181764	0.915578236	1436845_at	*Axin2*
1741	-0.272225812	-1.207669602	0.344053198	1417409_at	*Jun*
32995	-0.320745097	-1.248975431	0.338574059	1448694_at	*Jun*
28826	0.001448836	1.001004761	0.98269741	1444519_at	*Lgr5*
35284	-0.01272021	-1.008855962	0.96171315	1450988_at	*Lgr5*
3636	0.270671496	1.206369196	0.331107416	1419304_at	*T*
4644	0.429942093	1.347179502	0.28178972	1420337_at	*Gbx2*
33883	0.733043422	1.662141749	0.344896614	1449582_at	*Cdx1*
253	0.100157776	1.07189068	0.545620612	1415921_a_at	*Tnfrsf19*
9519	0.148432793	1.108364796	0.451139341	1425212_a_at	*Tnfrsf19*
32448	0.016499704	1.011502373	0.94265723	1448147_at	*Tnfrsf19*
33779	0.008333558	1.005793097	0.833733354	1449478_at	*Mmp7*
10010	-0.00946854	-1.006584676	0.910097025	1425703_at	*Ppard*
24104	-0.167938773	-1.123452224	0.136555917	1439797_at	*Ppard*
10719	0.062984217	1.044624334	0.66564989	1426412_at	*Neurod1*
10720	0.080008756	1.057024456	0.554530867	1426413_at	*Neurod1*
5419	0.112143264	1.080832726	0.666845523	1421112_at	*Nkx2-2*
22858	-0.749572674	-1.681294758	0.14571802	1438551_at	*Neurog1*
35132	0.040716663	1.028624672	0.798325162	1450836_at	*Neurog1*
1751	-0.125847545	-1.091148565	0.514050518	1417419_at	*Ccnd1*
1752	-0.22043166	-1.165082131	0.125036228	1417420_at	*Ccnd1*
32999	-0.31180544	-1.241260085	0.006021336	1448698_at	*Ccnd1*
454	-0.479296827	-1.39406403	0.032819728	1416122_at	*Ccnd2*
455	-0.461771304	-1.37723171	0.041111246	1416123_at	*Ccnd2*

456	-0.518002713	-1.431971434	0.041384851	1416124_at	*Ccnd2*
14343	-0.49468802	-1.409016025	0.036310447	1430127_a_at	*Ccnd2*
19052	-0.4226797	-1.340414966	0.054573644	1434745_at	*Ccnd2*
32530	-0.493894403	-1.408241148	0.020480653	1448229_s_at	*Ccnd2*
40252	-0.493286247	-1.40764764	0.033099878	1455956_x_at	*Ccnd2*
239	-0.18298923	-1.135233627	0.18261158	1415907_at	*Ccnd3*
23112	-0.034170701	-1.02396805	0.745531307	1438805_at	*Ccnd3*
28630	-0.053213277	-1.037573312	0.381066095	1444323_at	*Ccnd3*

Genes upregulated by canonical Wnt signaling, but not known to be directly controlled by LEF/TCF/beta-catenin

Number	$\log_2$ fold change	Fold change	*P*-value	Probe set ID	Gene symbol
10229	-0.031643168	-1.022175677	0.834837614	1425922_a_at	*Mycn*
10230	-0.074839608	-1.053243935	0.370151246	1425923_at	*Mycn*
2119	0.157889939	1.115654208	0.272391433	1417787_at	*Dkkl1*
9257	-0.372285003	-1.294401337	0.171519097	1424950_at	*Sox9*
18196	-0.069787667	-1.0495622	0.580000591	1433889_at	*Sox9*
35834	-0.277903713	-1.212431897	0.177249344	1451538_at	*Sox9*
5964	0.374839047	1.296694882	0.05674946	1421657_a_at	*Sox17*
13484	0.468411795	1.383585496	0.095193624	1429177_x_at	*Sox17*
3536	-0.141376469	-1.102956941	0.252686238	1419204_at	*Dll1*
3065	-0.14528704	-1.105950673	0.327187884	1418733_at	*Twist1*

Table S2. STF reporter assay of canonical Wnt signaling
Data are the averages of three transfections and have been normalized for the cotransfected *Renilla* luciferase.

Fz+Lrp5	
Fz1	0.48
Fz2	0.37
Fz3	0.76
Fz4	2.54
Fz5	0.46
Fz6	0.7
Fz7	1.02
Fz8	0.85
Fz9	16.3
Fz10	0.26

Wnt+Lrp5	
Wnt1	140.8
Wnt2	4.08
Wnt2b	0.19
Wnt3	11.18
Wnt3a	13.57
Wnt4	0.35
Wnt5a	0.18
Wnt5b	0.14
Wnt6	0.204
Wnt7a	0.715
Wnt7b	2.082
Wnt8a	0.342
Wnt8b	0.351
Wnt9a	0.193
Wnt9b	1.329
Wnt10a	0.356
Wnt10b	14.706
Wnt11	0.18
Wnt16	0.583

Wnt+Fz+Lrp5 (not normalized for Wnt+Lrp5 and Fz+Lrp5)

	Fz1	Fz2	Fz3	Fz4	Fz5
Wnt1	92.91	82.82	140.46	87.6	107.9
Wnt2	11.38	25.87	1.74	27.06	42.54
Wnt2b	1.43	1.26	1.18	6.69	12.39
Wnt3	102.8	75.06	5.22	44.43	76.9
Wnt3a	102	63.5	14.11	32.8	63.4
Wnt4	0.72	0.44	0.37	2.56	0.51
Wnt5a	0.59	0.41	0.27	4.1	1.2
Wnt5b	0.68	0.68	0.7	7.14	1.21
Wnt6	5.39	2.87	0.45	13.09	18.59
Wnt7a	9.97	8.44	1.15	9.07	75.82
Wnt7b	37	27.9	2.79	40.35	152.3

Wnt8a	4.49	4.49	0.92	11.75	28.72
Wnt8b	0.98	2	1.34	9.49	21.01
Wnt9a	0.89	0.47	0.58	2.01	0.64
Wnt9b	6.77	2.79	1.26	27.35	68.8
Wnt10a	3.43	1.65	1.22	9.08	8.03
Wnt10b	29.61	34.37	18.38	47.73	53.23
Wnt11	0.44	0.56	1.27	17.5	0.82
Wnt16	0.77	0.87	0.96	8.58	1.27

	Fz6	Fz7	Fz8	Fz9	Fz10
Wnt1	98.8	57.89	170.79	129.5	170.1
Wnt2	1.05	25.43	72.58	55.23	7.46
Wnt2b	0.86	2.69	22.4	18.23	0.94
Wnt3	4.19	76.14	49.12	37.36	18.94
Wnt3a	21.4	79.36	55.09	37.73	39.17
Wnt4	0.9	0.98	0.5	11.18	0.37
Wnt5a	0.82	1.02	0.93	15.34	0.19
Wnt5b	1.75	1.49	1.15	17.3	0.27
Wnt6	0.85	3.85	17.8	9.83	1.91
Wnt7a	0.97	13.39	55.36	23.5	1.15
Wnt7b	1.04	35.95	118.9	49.3	4.38
Wnt8a	0.89	6.94	39.55	22.13	2.29
Wnt8b	0.94	2.74	47.96	17.9	0.49
Wnt9a	0.88	0.92	1.08	13.04	0.63
Wnt9b	1.96	4.85	37.51	126.61	15.7
Wnt10a	0.84	5.16	2.73	20.21	0.78
Wnt10b	5.2	36.19	36	58.5	32.03
Wnt11	0.83	1.64	1.9	18.04	0.64
Wnt16	0.8	2.26	0.74	32.25	0.77

Wnt+Fz+Lrp5 (normalized for Wnt+Lrp5 and Fz+Lrp5)

	Fz1	Fz2	Fz3	Fz4	Fz5
Wnt1	0.85	0.76	1.03	0.83	1.03
Wnt2	3.22	6.49	0.49	4.45	11.41
Wnt2b	2.03	2.07	1.37	2.83	18.46
Wnt3	11.98	7.68	0.56	4.05	8.55
Wnt3a	8.13	5.71	0.83	2.15	5.13
Wnt4	0.82	0.51	0.37	0.99	0.53
Wnt5a	0.89	0.64	0.44	1.3	1.12
Wnt5b	0.95	1.12	0.79	2.95	1.7
Wnt6	9.45	6.07	0.64	11.28	34.93
Wnt7a	4.39	5.6	0.73	1.51	46.97
Wnt7b	12.45	10.86	0.87	5.63	51.27
Wnt8a	6.27	6.41	0.84	4.81	40.56
Wnt8b	1.34	2.98	1.23	2.95	27.1
Wnt9a	1.58	0.95	0.64	0.75	0.99
Wnt9b	4.03	1.95	0.75	8.99	38.78
Wnt10a	4.73	2.59	1.08	2.83	10.06
Wnt10b	4.52	2.75	1.28	2.92	4.37
Wnt11	0.91	1.28	1.51	7.03	1.28

Wnt16	0.85	0.98	0.81	3.35	1.13

	Fz6	Fz7	Fz8	Fz9	Fz10
Wnt1	0.7	0.53	1.34	1.05	1.34
Wnt2	0.28	5.21	17.63	2.81	1.93
Wnt2b	0.66	2.11	21.16	1.49	1.96
Wnt3	0.95	8.11	6.09	1.3	2.08
Wnt3a	0.91	5.67	4.28	1.5	3.06
Wnt4	0.7	0.78	0.39	0.81	0.53
Wnt5a	0.76	0.81	0.77	1.12	0.42
Wnt5b	22.25	1.15	0.98	1.15	0.72
Wnt6	0.38	5.38	20.4	1.11	4.5
Wnt7a	1.11	4.74	22.66	0.87	1.25
Wnt7b	1.51	8.27	30.13	1.57	1.81
Wnt8a	0.89	5.72	32.45	1.54	3.72
Wnt8b	1.23	1.83	35.82	1.09	1.03
Wnt9a	1.02	0.82	0.92	0.87	1.43
Wnt9b	0.89	2.15	18.12	8.39	13.26
Wnt10a	0.63	3.77	2.23	1.37	1.63
Wnt10b	0.8	2.42	3.13	1.89	2.54
Wnt11	1.06	1.29	1.41	1.2	1.68
Wnt16	0.48	1.67	0.42	2.21	0.86